AWARD NUMBER: W81XWH-22-1-0382

TITLE: Defining the Role of B Cells in CNS Demyelination

PRINCIPAL INVESTIGATOR: Dr. Robert Miller, PhD

CONTRACTING ORGANIZATION: George Washington University

REPORT DATE: AUGUST 2023

TYPE OF REPORT: Annual

PREPARED FOR: U.S. Army Medical Research and Development Command
Fort Detrick, Maryland 21702-5012

DISTRIBUTION STATEMENT: Approved for Public Release;
Distribution Unlimited

The views, opinions and/or findings contained in this report are those of the author(s) and should not be construed as an official Department of the Army position, policy or decision unless so designated by other documentation.

REPORT DOCUMENTATION PAGE

Form Approved
OMB No. 0704-0188

Public reporting burden for this collection of information is estimated to average 1 hour per response, including the time for reviewing instructions, searching existing data sources, gathering and maintaining the data needed, and completing and reviewing this collection of information. Send comments regarding this burden estimate or any other aspect of this collection of information, including suggestions for reducing this burden to Department of Defense, Washington Headquarters Services, Directorate for Information Operations and Reports (0704-0188), 1215 Jefferson Davis Highway, Suite 1204, Arlington, VA 22202-4302. Respondents should be aware that notwithstanding any other provision of law, no person shall be subject to any penalty for failing to comply with a collection of information if it does not display a currently valid OMB control number. **PLEASE DO NOT RETURN YOUR FORM TO THE ABOVE ADDRESS.**

1. REPORT DATE	2. REPORT TYPE	3. DATES COVERED
AUGUST 2023	Annual	1 Aug 2022 – 31 Jul 2023

4. TITLE AND SUBTITLE
Defining the role of B cells in CNS demyelination

5a. CONTRACT NUMBER
W81XWH-22-1-0382

5b. GRANT NUMBER
W81XWH-22-1-0382

5c. PROGRAM ELEMENT NUMBER

6. AUTHOR(S)
Robert H. Miller, Yusra Islam, Julie J. Ahn

E-Mail: rhm3@gwu.edu

5d. PROJECT NUMBER

5e. TASK NUMBER

5f. WORK UNIT NUMBER

7. PERFORMING ORGANIZATION NAME(S) AND ADDRESS(ES)

George Washington University
2300 I St. NW, Ross Hall 735
Washington, DC 20037

8. PERFORMING ORGANIZATION REPORT NUMBER

9. SPONSORING / MONITORING AGENCY NAME(S) AND ADDRESS(ES)

U.S. Army Medical Research and Development Command
Fort Detrick, Maryland 21702-5012

10. SPONSOR/MONITOR'S ACRONYM(S)

11. SPONSOR/MONITOR'S REPORT NUMBER(S)

12. DISTRIBUTION / AVAILABILITY STATEMENT

Approved for Public Release; Distribution Unlimited

13. SUPPLEMENTARY NOTES

14. ABSTRACT

This project is designed to evaluate the effects of CNS B cells on glial cells and myelin integrity in demyelinating disease, using selective cell depletion approaches including a novel transgenic animal model termed CD19Cre-iCP9. Clinical studies in multiple sclerosis show the effectiveness of B cell depletion therapies, including rituximab and ocrelizumab, although the underlying mechanisms are not well understood. In preliminary studies, using a combination of EAE and the CD19Cre-iCP9 models, we depleted B cells specifically in the CNS and found a stabilization of disease and reduction in myelin and axonal damage in the spinal cord. In the current studies, we have systemically depleted B cells in the EAE model and demonstrated rapid functional recovery. Analyses of early changes in gene expression in astrocytes and microglia by RNA sequencing following B cell depletion suggest that inflammatory pathways in astrocytes and changes in microglial-neuron interactions drive disease progression. By contrast, improvements in neurovascular functioning are associated with recovery after B cell depletion. These unexpected findings have the potential to change our understanding of the role of B cells during disease and myelin repair, and in the coming year, we will shift our focus to understanding the B cell-neurovascular unit interactions using the CNS selective B cell depletion model, evaluating molecular mechanisms and ultrastructural characterization of myelin repair.

15. SUBJECT TERMS
Multiple sclerosis, astrocytes, microglia, EAE, myelin, B cells

16. SECURITY CLASSIFICATION OF:			17. LIMITATION OF ABSTRACT	18. NUMBER OF PAGES	19a. NAME OF RESPONSIBLE PERSON
a. REPORT	b. ABSTRACT	c. THIS PAGE			USAMRDC
U	U	U	UU	26	19b. TELEPHONE NUMBER *(include area code)*

TABLE OF CONTENTS

	Page
1. Introduction	4
2. Keywords	4
3. Accomplishments	4
4. Impact	8
5. Changes/Problems	9
6. Products	9
7. Participants & Other Collaborating Organizations	10
8. Special Reporting Requirements	11
9. Appendices	12

INTRODUCTION

Multiple sclerosis (MS) is characterized by localized lesions in the brain and spinal cord where myelin, the fatty insulation around axons, is lost. Myelin is produced by cells called oligodendrocytes and when it is lost or damaged axons fail to transmit information, resulting in compromised function. The causes of MS are not well defined. However, in many cases, early in the disease while there is robust remyelination and functional recovery this ultimately fails as the disease progresses. The reasons for remyelination failure are not well understood although the presence of oligodendrocyte precursors in chronic lesions suggests that it is not a lack of new cells but rather changes in the environment of the lesion that limit the ability of these cells to mature into myelinating oligodendrocytes. For many years MS was considered a T-cell mediated disease, however, the more recent studies showing that systemic B cell depletion is highly effective in early relapsing remitting MS has demonstrated a critical role for B cells in the disease. Little is known, however, about how B cells drive disease and how their removal facilitates recovery. In this project, we have used *in vivo* and *in vitro* approaches to characterize the interactions of B cells with neural cells in the CNS. Such information is essential since systemic B cell depletion is less effective later in the disease and B cells remain present in the brain and spinal cord where they may continue to inhibit repair. Consistent with this idea, in exciting new studies, we have found that in a model of chronic MS, selective depletion of CNS B cells in the brain and spinal cord results in functional benefit and that systemic B cell depletion results in rapid functional improvement that is associated with distinct changes in CNS glial gene expression. In this proposal, we test the hypothesis that a major obstacle to myelin repair are changes in the glial environment that result from the presence of B cells in the brain and spinal cord. We will build on our recent observations that functional recovery following B cell depletion is associated with changes in the neurovascular unit and, using an animal model we have developed to selectively deplete B cells in the brain and spinal cord, examine the mechanism and extent of changes in the neurovascular unit and myelin repair following localized B cell depletion. Such studies will provide novel insights into potential therapeutic avenues for MS treatment.

KEYWORDS

Multiple sclerosis, astrocytes, microglia, EAE, myelin, B cells

ACCOMPLISHMENTS

1. **What were the major goals of the project?**

   Major goals of the project listed in the approved SOW with completion dates or percent completed:

Specific Aim 1: To determine the effects of CNS specific B cell depletion on myelin repair and functional recovery in EAE.	**% Complete**	**Completion date**
Major Task 1: Expand animal colony, refine selective depletion of CNS B cells and assay functional recovery, number of mature oligodendrocytes and levels of remyelination by EM.	50	
Subtask 1: Obtain IACUC and ACURO approval for studies. Initiate the breeding of the CreCD19-iCP9 animals and grow the colony.	100	
Subtask 2: Induce MOG1-125 EAE and treat with CID to selectively. Deplete CNS B cells.	50	
Subtask 3: Perform functional studies and record outcomes. Sacrifice animals, prepare tissue for phenotypic analysis of innate immune cells. Prepare samples for ultrastructural analyses of remyelination and analyze data.	50	
Specific Aim 2: Identifying changes in CNS glial cell phenotypes and cytokine expression in response to CNS B cell depletion.		

Major Task 2: Characterization of CNS glial reactivity and prepare RNA samples.	70	
Subtask 1: Deplete CNS B cells from EAE animals with CID delivery.	20	
Subtask 2: Prepare purified populations through immuno-isolation protocols and isolate RNA. Initiate single cell RNA studies. Prepare samples and develop protocols.	75	
Major Task 3: Analyze data and prepare publication.	50	
Subtask 1: Generate RNA samples from purified cell population. Send purified RNA for sequencing and analyze data to identify affected signaling pathways.	75	
Subtask 2: Conduct pathway analysis on purified RNA samples to identify pathways altered by CNS B cell depletion. Interrogate RNA for altered pathway analysis. Quantify cellular responses to B cell depletion.	75	
Subtask 3: Write and submit 1-2 manuscripts reporting changes in phenotypic cell profiles and alterations in CNS cell signaling pathways.	50	1st manuscript submitted July 2023

2. What was accomplished under these goals?

Specific Aim 1: To determine the effects of CNS specific B cell depletion on myelin repair and functional recovery in EAE

Major Task 1: Expand animal colony, refine selective depletion of CNS B cells and assay functional recovery, number of mature oligodendrocytes and levels of remyelination by EM.

- CD19Cre-iCP9 animals were treated with tamoxifen and induced with EAE to deplete B cells in the CNS. Further validation studies were done to determine efficacy of CID treatment. The number of B220+ B cells were quantified in the spleen, cervical draining lymph nodes, and spinal cords. No significant differences in B cell numbers were observed in the spleen and lymph nodes after CID treatment, but there was a significant loss of B cells in the spinal cord (Fig. 1).
- Toluidine blue staining of semi-thin sections revealed increased numbers of axons with collapsed myelin sheaths in vehicle control animals compared to CID treated mice (Fig. 2).

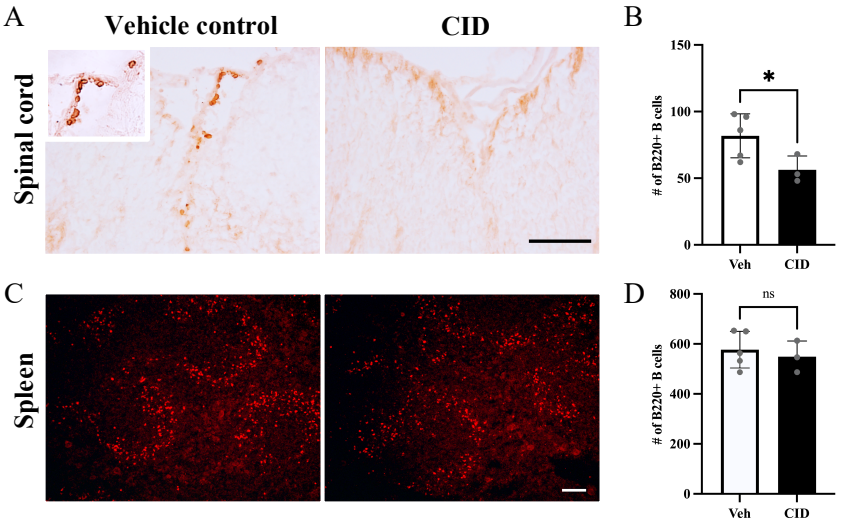


Fig. 1 CNS CID administration depletes CNS specific B cells. A) B220+ B cells that penetrate EAE spinal cords are depleted following CID treatment. B) Quantification of the number of B220+ B cells in 10 µm sections of the spinal cord in vehicle and CID treated EAE animals. C) No detectable change in B cells in the spleen were found between vehicle and CID treated EAE animals. D) Quantification of the number of B220+ B cells in one 10µm section of the spleen. Scale bars: A = 50µm, C=100µm. Data represent the mean ± SD. *$p<0.05$; compared with the corresponding control, in 3-5 animals per treatment group (Student's *t* test).

Specific Aim 2: Identifying changes in CNS glial cell phenotypes and cytokine expression in response to CNS B cell depletion

Major Task 2: Characterization of CNS glial reactivity and prepare RNA samples

- To support single cell sequencing studies and evaluate population-level metrics of cells affected by B cell treatment in EAE, systemic B cell depletion was performed by intraperitoneal injections of anti-CD19/anti-B220 when animals reached a score of 2.5 and RNA from astrocytes and microglia were analyzed 3 days following treatment.
- Protocols were optimized to isolate viable astrocytes and microglia from EAE spinal cords. A total of 10 astrocyte and 10 microglia RNA samples were extracted from EAE spinal cords. RNA was isolated 3 days following B cell depletion to analyze immediate glial responses to B cell depletion.

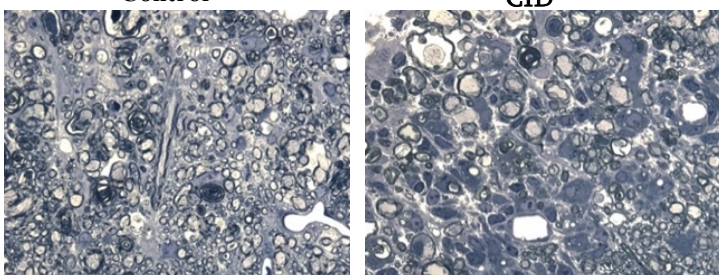


Fig. 2 CNS B cell depletion reduces myelin and axonal damage. Toluidine blue stained semi-thin sections of spinal cords show increased number of axons with collapsed myelin sheaths in vehicle control animals compared to CID treated mice.

We found that myelin removal and isolation of pure, viable cells resulted in the highest quality RNA when combining mechanical and enzymatic dissociation of spinal cord tissues with magnetic cell sorting of astrocytes and microglia. Validation of these methods was done at the George Washington University Genomics Core. Using this protocol, we were able to achieve the cell purity and quantity necessary for purified cell sequencing analysis.

Major Task 3: Analyze data and prepare publication

- RNA samples from astrocytes and microglia were sequenced at Q^2 Solutions Genomics (North Carolina, USA). A total of 20 total RNA samples were analyzed using the Illumina TruSeq Total RNA platform and Q^2 RNAv10 pipeline.
- Initial comparison analyses by Limma-Voom differential were performed at Q^2 Solutions Genomics (Table 1). Comparisons included untreated EAE vs treated EAE, healthy control vs treated EAE, and healthy controls vs untreated EAE for astrocytes and microglia.

Table 1 Number of differentially expressed genes in different comparisons

Comparison	Reference Group	Comparator Group	(1) Num Sig. Adj. P < 0.05	(2) (1) + |L2FC|>0.25	(3) (2) + Homologous
Comparison 1	Astrocytes Untreated EAE	Astrocytes Treated EAE	64	64	57
Comparison 2	Astrocytes Healthy Controls	Astrocytes Treated EAE	4925	4925	3272
Comparison 3	Astrocytes Healthy Controls	Astrocytes Untreated EAE	8150	8150	5534
Comparison 4	Microglia Untreated EAE	Microglia Treated EAE	367	367	319
Comparison 5	Microglia Healthy Controls	Microglia Treated EAE	6132	6132	4561
Comparison 6	Microglia Healthy Controls	Microglia Untreated EAE	10578	10578	7379

*Data from Ahn, JJ, et al., 2023 (Appendix 1).

- Further pathway analyses were performed using Ingenuity Pathway Analysis (IPA) and Gene Ontology (GO) enrichment analysis. GO analysis revealed astrocyte inflammatory pathways are over-represented in EAE animals compared to healthy controls (Fig. 3). Top GO terms included cytokine receptor activity, immune receptor activity, and cytokine binding. In microglia, extracellular matrix organization, transmission across chemical synapses, and postsynaptic signal transmission were over-represented in EAE compared to healthy controls and IPA analysis revealed predicated inhibition of CREB signaling in neurons and synaptogenesis, suggesting that microglia play a critical role in modulating neuronal activity in EAE.
- Three days following B cell depletion, astrocyte inflammatory responses were not primarily responsible for the improvement in clinical symptoms (Fig. 4). IPA analysis revealed astrocyte genes associated with

neurovascular coupling signaling were upregulated in B cell depleted compared to control EAE animals. The top IPA pathways in microglia in EAE were reversed after B cell depletion; there was predicated activation CREB signaling in neurons.

- We have submitted a manuscript including the RNA analyses to *Neurobiology of Disease*, and it is under review. Another manuscript is being prepared to include changes in oligodendrocyte and oligodendrocyte precursor populations as a result of B cell depleting treatment in EAE.

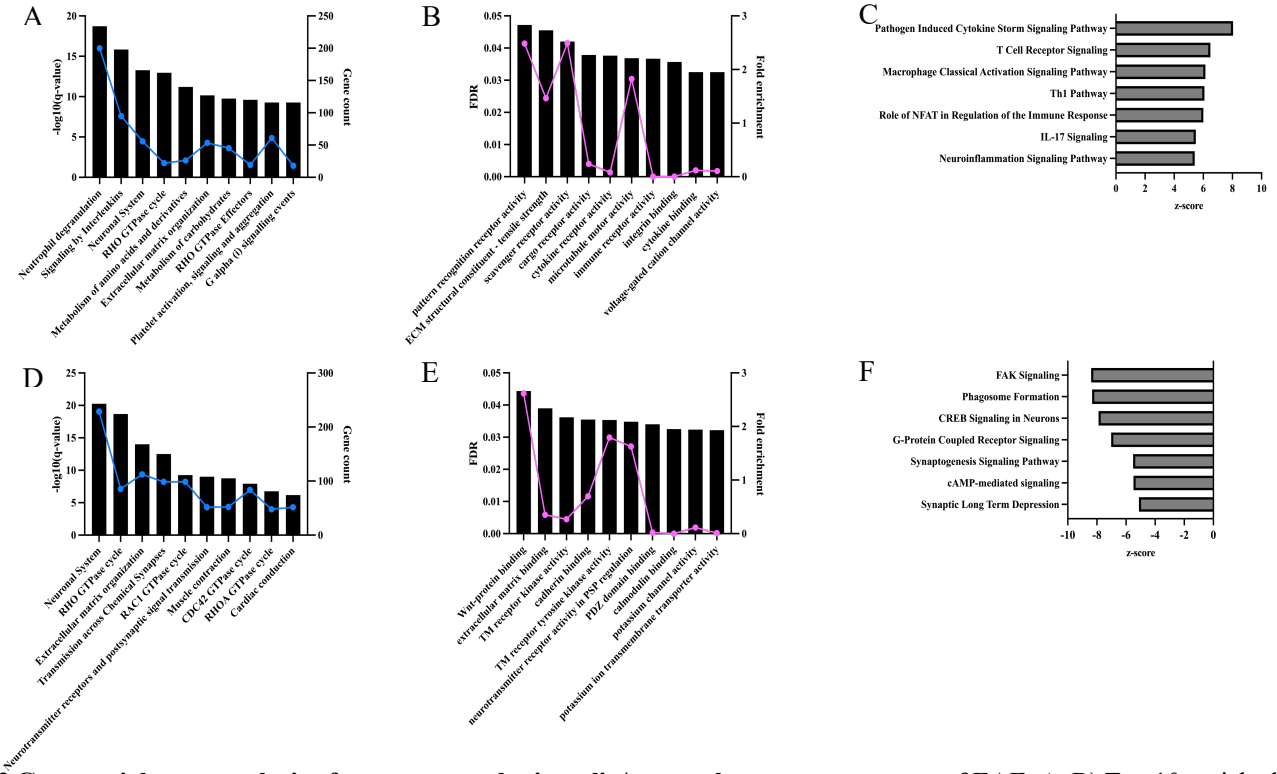


Fig. 3 Gene enrichment analysis of astrocytes and microglia/macrophages at acute stage of EAE. A, B) Top 10 enriched GO terms and C) top canonical pathways by Ingenuity Pathway Analysis of spinal cord astrocytes from EAE animals, normalized against healthy controls. D, E) Top 10 enriched GO terms and F) top canonical pathways by Ingenuity Pathway Analysis of spinal cord microglia from EAE animals, normalized against healthy controls. A, D) Bars show gene counts and lines show -log10(q-value) of top 10 biological processes. Q-values are FDR-adjusted p-values or the minimum FDR at which values are deemed significant. B, E) Bars show fold enrichment and lines show FDR of top 10 molecular functions. FDR is the rate that significant features are found to be truly null. FDR $p<0.05$. Data from Ahn, JJ, et al., 2023 (Appendix 1).

Goals not met: We are continuing to expand the transgenic CD19Cre-iCP9 animal colony to reach the intended sample size of 7 per group (CID vs vehicle control at two timepoints). However, we have had general breeding issues in the animal colonies, unrelated to this CD19Cre-iCP9 strain. We have been replacing breeders with younger animals and have been adding additional breeding pairs to increase animal numbers. We have prepared samples for electron microscopy to perform ultrastructural analysis to assess remyelination and oligodendrocyte death. We expect these studies to be completed by the end of 2023.

3. What opportunities for training and professional development has the project provided?

Nothing to Report.

4. How were the results disseminated to communities of interest?

We have given a number of seminars at our home and other institutions and are preparing manuscripts for publication.

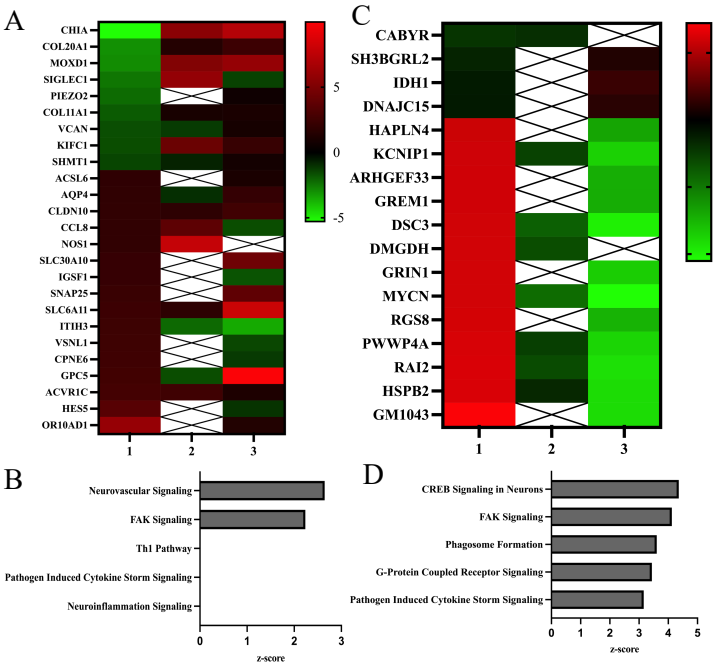


Fig. 4 Differentially expressed genes and canonical pathways in spinal cord astrocytes and microglia/macrophages after B cell depletion. A) Top differentially expressed genes in astrocytes isolated from B cell depleted EAE versus control EAE animals (column 1) and corresponding fold changes in astrocytes isolated from B cell depleted EAE versus healthy controls (column 2) and control EAE versus healthy controls (column 3). B) Canonical pathways for astrocytes of B cell depleted EAE versus control EAE animals showing neurovascular and FAK signaling pathways to be activated and no differences in immune related pathways. C) Top differentially expressed genes in microglia/macrophages isolated from B cell depleted EAE versus control EAE animals (column 1) and corresponding fold changes in microglia/macrophages isolated from B cell depleted EAE versus healthy controls (column 2) and control EAE versus healthy controls (column 3). D) Top canonical pathways in microglia/macrophages of B cell depleted EAE versus control EAE animals showing predicted activation of CREB signaling in neurons and GPCR signaling. Data from Ahn, JJ, et al., 2023 (Appendix 1).

5. **What do you plan to do during the next reporting period to accomplish the goals?**

During the next reporting period, we plan to follow up on the finding of changes to the neurovascular unit following systemic B cell depletion. We will analyze samples for remyelination and oligodendrocyte/oligodendrocyte precursor cell numbers and morphology by electron microscopy. We also plan to increase our animal colony to generate additional transgenic animals. Using the transgenic animals, we plan to directly test the hypothesis that B cell-CNS glia interactions mediate the demyelinating pathology and their depletion accounts for the rapid recovery through distinct cellular and molecular pathways.

IMPACT

1. **What was the impact on the development of the principal discipline(s) of the project?**

It is widely known that B cell depletion therapy in MS is effective in relapsing-remitting and some progressive stages of disease. Currently, it is unclear how B cell depletion is able to ameliorate disease and improve neurologic function. However, due to the pro-inflammatory profile of B cells, many believe that the improvement in clinical outcomes was due to the loss of this population of neurotoxic B cells. Our preliminary RNA analyses revealed that B cells may modulate glial cells during progression of disease as well as recovery from disease after B cell depleting treatments. Therefore, rather than a direct effect of B cells on myelin or neuronal function, astrocytes and microglia appear to mediate recovery through their impact on neurovascular and neuronal function. These studies will likely change our understanding of MS pathogenesis. Long-term, this project may provide novel targets for therapies that do not target critical antibody-producing B cells.

2. **What was the impact on other disciplines?**

It is possible that our data will provide new insights in B cells, or subsets of B cells in other autoimmune diseases.

3. **What was the impact on technology transfer?**

Nothing to Report.

4. **What was the impact on society beyond science and technology?**

   Nothing to Report.

CHANGES/PROBLEMS

1. **Changes in approach and reasons for change**

   We had proposed to use CD19Cre-iCP9 transgenic animals to ablate B cells in the CNS after EAE induction. However, we have encountered general breeding issues, not specific to this strain, and have been unable to generate a sufficient number of animals to complete the proposed set of experiments thus far. While continuing to breed transgenic animals, we optimized cell sorting and RNA isolation protocols for EAE spinal cord tissues. We were able to sequence 20 total RNA samples with bulk RNA sequencing. We decided to perform this set of bulk RNA sequencing experiments to complement the proposed single cell sequencing analysis. The bulk RNA sequencing data provided valuable insight into specific pathways that may be affected as a result of B cell depletion. Additionally, B cell depletion for bulk RNA sequencing was done by intraperitoneal injections using antibodies rather than CID treatment to minimize cost and need for transgenic animals. These results have provided us with an unexpected insight into the interactions between B cells and CNS neural cells that we will test in the coming year using the CNS B cell deletion model. We will deemphasize the single cell RNA studies in order to test the hypothesis that a primary target of B cells in the CNS is the neurovascular unit.

2. **Actual or anticipated problems or delays and actions or plans to resolve them**

   We are continuing to expand the size of the mouse colony and add new breeders to generate enough transgenic animals. We have replaced breeders with younger animals and have added additional breeding cages. We anticipate that we will have sufficient animals to complete the proposed experiments in this next reporting period.

3. **Changes that had a significant impact on expenditures**

   The studies in the last year have been highly productive in spite of difficulties with the transgenic animal colony. We have successfully leveraged endowment funds and individual funding to ensure the continued success of the project.

4. **Significant changes in use or care of human subjects, vertebrate animals, biohazards, and/or select agents**

   Nothing to Report.

5. **Significant changes in use or care of human subjects**

   Nothing to Report.

6. **Significant changes in use or care of vertebrate animals.**

   Nothing to Report.

7. **Significant changes in use of biohazards and/or select agents**

   Nothing to Report.

PRODUCTS

Journal publications:

1. Ahn JJ, Clarkson-Paredes C, Islam Y, Karl MT, and Miller RH. B cell depletion modulates astrocyte and microglia responses, enhances blood vessel integrity, and reduces immune cell infiltration in a model of multiple sclerosis. *Neurobiology of Disease,* 2023. (Under review, Acknowledgement of federal support: Yes)
2. Ahn, Julie; Islam, Yusra; Miller, Robert (2023), "Transcriptomic profiling of EAE astrocytes and microglia +/- B cell depletion", Mendeley Data, V1, doi: 10.17632/98ph95fw6n.1 (Embargo until Oct. 10, 2023; Acknowledgement of federal support: Yes)

PARTICIPANTS & OTHER COLLABORATING ORGANIZATIONS

1. **What individuals have worked on the project?**

   We have added Julie Ahn to the project. She is a postdoctoral associate and has funding support through Dr. Miller's endowment funds. She has contributed 6 months to the project, directing the RNA sequencing and histological studies.

Name:	Robert H. Miller
Project Role:	Principal investigator
Researcher Identifier (e.g. ORCID ID):	0000-0001-9050-4154
Nearest person month worked:	No change.
Contribution to Project:	No change.
Funding Support:	No change.

Name:	Yusra Islam
Project Role:	Research associate
Researcher Identifier (e.g. ORCID ID):	0000-0001-7570-7850
Nearest person month worked:	No change.
Contribution to Project:	No change.
Funding Support:	No change.

Name:	Julie Ahn
Project Role:	Postdoctoral associate
Researcher Identifier (e.g. ORCID ID):	0000-0001-5168-6717
Nearest person month worked:	6 months
Contribution to Project:	RNA sequencing and histology studies
Funding Support:	Robert H. Miller endowment funds

2. **Has there been a change in the active other support of the PD/PI(s) or senior/key personnel since the last reporting period?**

   The support to the PI (Miller) has not changed during the award. Dr. Julie Ahn, who was supported on a separate graduate fellowship and is now supported from Dr. Miller's endowment funds, has been a major contributor to the project and has been an essential member of the team.

3. **What other organizations were involved as partners?**

   Nothing to Report.

SPECIAL REPORTING REQUIREMENTS

Nothing to Report.

APPENDICES:

APPENDIX 1:

INTRODUCTION

The pathological hallmark of multiple sclerosis (MS) is the presence of central nervous system (CNS) infiltrating peripheral immune cells and the reactivity of astrocytes and microglia within and around demyelinating lesions, resulting in CNS injury. In the intact CNS, astrocytes provide a range of functional support to neurons, including glutamate homeostasis, modulation of synapses, and regulation of extracellular ions. Astrocytes also play a pivotal role in the maintenance of the blood-brain barrier (BBB) that regulates movement of materials and cells between the circulatory system and CNS parenchyma [1,2]. In MS, reactive gliosis induced BBB disruption has a detrimental effect on the CNS, leading to an influx of peripheral immune cells and soluble factors and subsequent neuronal damage [3]. Microglia, a heterogenous cell population, perform immune surveillance and modulate neuronal function in the absence of insults. In the setting of demyelinating disease, the role of microglia in MS is less well defined; it is unclear whether phagocytic microglia within lesions are a cause of myelin damage or promote repair through myelin debris clearance [4,5]. In active demyelination, however, a pro-inflammatory microglia phenotype is common [6,7], which may contribute to inflammation in the CNS.

While pathological studies in MS have described a varying degree of immune cell infiltration in the CNS, a common feature is the presence of elevated numbers of T cells and B cells [8–12]. Some populations of B cells in MS patients have an aberrant pro-inflammatory profile, expressing a high level of pro-inflammatory proteins and a low level of anti-inflammatory cytokines compared to healthy controls [13,14]. Furthermore, the recent success of B cell targeted therapies, including rituximab and ocrelizumab, in both relapsing-remitting and progressive forms of MS, has highlighted the significance of B cells in the progression of disease [15,16]. The presence of pro-inflammatory B cells that secrete neurotoxic factors, together with the local reactivity of astrocytes and microglia, suggests a role for B cells in stimulating deleterious glial activity in demyelinating diseases such as MS.

The interactions between B cells and CNS glial cells are not well understood and, to begin to define the effects of B cells on glial responses in an inflammatory setting, we utilized a B cell depletion approach in a model of EAE that engages B cells. To assess changes in astrocytes and microglia that were influenced by the presence of B cells, cell and tissue morphology and gene expression were compared between control, EAE, and B cell depleted EAE samples. We show that B cell depletion at the acute phase of EAE, prior to peak disease when there is a high level of inflammatory infiltrates and glial reactivity, alters the progression of disease. To gain a clearer understanding of the effects of B cell depletion on astrocyte and microglia responses, we compared changes in astrocyte and microglia transcriptomes following EAE induction and after B cell depletion. We provide evidence that induction of EAE is associated with elevated astrocytic inflammatory pathways while the loss of B cells has a profound effect on cellular pathways involved in vasculature and neuronal function. These observations implicate B cells in promoting widespread inflammation through modulation of glial responses that directly impact the integrity of CNS vasculature.

METHODS

Animals

Female C57Bl/6J wild-type (WT) mice aged 12-16 weeks were obtained from The Jackson Laboratory and maintained at The George Washington University. All procedures were approved by The George Washington University Institutional Animal Care and Use Committee (Washington, D.C., USA) and complied with the National Research Council's *Guide for the Care and Use of Laboratory Animals*.

EAE induction

EAE was induced in 12-16 week old mice by active immunization with human recombinant myelin oligodendrocyte glycoprotein 1-125 (MOG_{1-125}) emulsified in Complete Freund's Adjuvant (CFA) (Hooke Laboratory), a B cell dependent EAE model. The antigen emulsion was administered subcutaneously at two sites: the midline of upper back and the midline of lower back. Two hours after MOG administration, 80 ng pertussis toxin in glycerol was administered intraperitoneally (i.p.). A second administration of 80 ng pertussis toxin was repeated 24 hours later. Clinical symptoms and scores were recorded daily based on the scoring guidelines provided by Hooke Laboratory. Animals were given a score 0-4 based on clinical observations: 1.0 limp tail; 1.5 limp tail and hind leg inhibition; 2.0 limp tail and hind leg weakness; 2.5 limp tail and dragging of hind limbs; 3.0 limp tail and complete paralysis of hind limbs; 3.5 limp tail and complete hind limb paralysis and unable to right itself; 4.0 limp tail, hind limb paralysis, and partial front limb paralysis.

B cell depletion

B cell depletion was performed by i.p. administration of 200 μg *InVivo*MAb anti-mouse CD19 (BioXCell) and 200 μg *InVivo*MAb anti-mouse B220 (BioXCell) [17] when animals reached a clinical score of 2.5 according to the scoring guidelines provided by Hooke

Laboratory (outlined above). Animals were either given a single dose (for RNA sequencing and electron microscopy) or one dose every 3 days (for immunohistochemistry).

Tissue collection

For immunohistochemistry (IHC), the spinal cord and spleen were harvested 20 days after symptom onset. Animals were anesthetized using Avertin (12.5 mg/mL of 2,2,2 Tri-bromoethanol, 2.5% 2-methyl-2-butanol in water). Cardiac perfusion was performed with cold 1X phosphate-buffered saline (PBS) to remove peripheral blood mononuclear cells (PBMCs) then 4% paraformaldehyde (PFA) to fix tissues. Tissues were removed and post-fixed in 4% PFA overnight. Tissues were transferred to 30% sucrose for 24 hours then embedded in Optimal Cutting Temperature (OCT) Compound (Fisher Scientific) and sectioned at 10 μm thickness.

For semi-thin section and electron microscopy analysis, spinal cords were dissected 3 days following B cell depletion. Animals were anesthetized using Avertin, and cardiac perfusion was performed using ice-cold 1X PBS and electron microscopy (EM) fixative (4% PFA, 2% glutaraldehyde, 0.1 M Na Cacodylate). Spinal cords were dissected, chopped into pieces less than 2 mm in length, fixed in EM fixative overnight at 4°C, and washed 3 times with 10 mL of 0.1 M Na Cacodylate buffer allowing 5 minutes per wash. Samples were post-fixed with 1% OsO4 diluted in ddH_2O two times for 3 hours at room temperature then samples washed 3 times for 15 minutes with ddH_2O. Samples were stored in 1% uranyl acetate solution overnight, washed with ddH_2O and dehydrated through 30%, 50%, 70%, 95%, and 100% ethanol, followed by 100% propylene oxide. Samples embedded in Epon 814 were cut at 500 nm thickness and stained with toluidine blue.

Glial cell isolation

Microglia and astrocytes were isolated 3 days following B cell depletion as previously described [18]. Animals were anesthetized using Avertin, and cardiac perfusion was performed using sterile cold tissue dissociation buffer (1X Dulbecco's phosphate-buffered saline (DPBS) supplemented with Ca2+/ Mg2+/ 0.2% glucose) to remove PBMCs. The spinal cord was removed by hydraulic extrusion with cold tissue dissociation buffer. Meninges were removed, and the spinal cord was chopped into 2-3mm pieces. Enzymatic dissociation was performed for 30 min at 37 °C using the Adult Brain Dissociation Kit (Miltenyi Biotec) according to the manufacturer's protocol. After enzymatic dissociation, 350 μL of 0.46 mg/mL DNAse I (Sigma-Aldrich) in Minimum Essential Medium (MEM; Corning) then cold Dulbecco's minimum essential medium (DMEM)/0.5% fetal bovine serum (FBS) were added. Dissociated tissues were triturated using a wide-bore borosilicate glass pipet and larger tissue aggregates removed using a 30 μm filter. Myelin debris was removed with debris removal solution (Miltenyi Biotec), and cells washed with cold DMEM/0.5% FBS. CD11b and ACSA-2 microbeads (Miltenyi Biotec) were added to spinal cord cell suspensions, and sorting of astrocytes and microglia was done according to the manufacturer's protocol. Briefly, cells were incubated with the microbeads then individual populations isolated by positive selection. Purity and viability were evaluated by Trypan blue exclusion.

Glial cell – B cell co-cultures

Glial cells from neonatal animals were isolated for *in vitro* studies using P1-3 neonatal C57Bl/6 male and female mice. Briefly, brains were dissected and submerged in cold tissue dissociation buffer and the meninges removed. Tissues were chopped using a surgical scalpel and Neural Tissue Dissociation Kit with papain (Miltenyi Biotec) was used to enzymatically digest samples according to the manufacturer's protocol. Briefly, samples were digested in the enzymes for 20 minutes at 37 °C with gentle swirling every 5 minutes. Samples were then triturated as described above and filtered through a 40 μm mesh funnel. The cell suspension was centrifuged at 300 x *g* for 10 minutes at room temperature. The supernatant was removed, and cells were resuspended in 70 μL of DPBS/0.5% bovine serum albumin (BSA) per 10^7 cells and 10 μL of FcR Blocking Reagent. Samples were incubated for 10 minutes at 4°C then A2B5+ oligodendrocyte precursor cells (OPCs) were isolated using anti-A2B5 microbeads (Miltenyi Biotec) according to the manufacturer's protocol. Cells were labeled with anti-A2B5 microbeads, washed with cold DPBS/0.5% BSA, and centrifuged at 300 x *g* for 10 minutes. The supernatant was aspirated and cells resuspended in 500 μL of DPBS/0.5% BSA. Cell suspensions were isolated using a MACS separator (Miltenyi) and plated on poly-L-lysine (PLL)-coated coverslips at a density of 10,000 cells per well in OPC base medium (DMEM/F12/B-27/2 mM L-Glutamine/100 U/mL Penicillin-Streptomycin). Two days later, the media was replaced with OPC proliferation media (OPC base medium with 20 ng/mL PDGF/20 ng/mL bFGF). Three days later, half of the wells were replaced with OPC proliferation media and the other half was replaced with astrocyte differentiation media (DMEM/F12/100 U/mL Penicillin-Streptomycin/10% FBS) to differentiate cells into mixed oligodendrocytes/astrocytes and purified astrocytes, respectively. Cells were cultured for 7 days before co-culturing with splenic B cells.

To isolate splenic B cells, the spleens from healthy and EAE (clinical score of 2.5) animals were dissected. After tissue harvest, spleens were mashed in a 70 μm cell strainer mesh placed in a Petri dish with ice-cold Hanks' balanced salt solution (HBSS; Corning). Filtered cells were centrifuged and supernatant discarded. Red blood cells were removed with 1 mL ACK lysing buffer (ThermoFisher) then washed with HBSS. B cells were purified by negative isolation using the MojoSort Mouse Pan B Cell Isolation Kit (BioLegend) according to the manufacturer's protocol. Unlabeled cells were collected and added to glial cell cultures at a density of 3,000 cells per well. While B cells require exogenous stimulation to avoid cell death [19], stimulation with serum components or *in vitro* mitogens changes B cell activity [20,21]. To minimize exogenous stimulation and cell death, B cells and glial cells were maintained in culture for 3 days in

low serum media (DMEM/100 U/mL Penicillin-Streptomycin/2% FBS). B cells cultured without glial cells were used as a control to assess cell viability.

Immunostaining

For fluorescence immunolabeling, 10 μm sections were blocked with 10% normal goat serum (NGS) and 0.3% Triton-X-100 in PBS for 1 hour at room temperature. Sections were incubated overnight at 4°C with rabbit anti-Iba1 (Wako), rabbit anti-GFAP (Dako), rat anti-MBP (Abcam), rat anti-B220 (BD), rabbit anti-albumin (Bio-rad), and rabbit anti-Claudin 5 (Cell Signaling). Sections were incubated with the appropriate secondary antibodies: Alexa Fluor 488 goat anti-rabbit IgG (Invitrogen), Alexa Fluor 488 goat anti-rat IgG (Invitrogen), Alexa Fluor 594 goat anti-rat IgG (Invitrogen), Alexa Fluor 594 goat anti-rabbit IgG (Invitrogen). Images were acquired using Leica DM5500B fluorescence microscope and processed in Photoshop.

Eriochrome cyanine-R staining

Frozen 10 μm sections were dried at room temperature for two hours. Slides were placed in acetone (Sigma-Aldrich) for 5 minutes then dried at room temperature for 15 minutes. Tissues were incubated in Eriochrome cyanine R solution (Sigma-Aldrich) for 30 minutes at room temperature, rinsed with running water, then differentiated in 5% ammonium ferric sulfate (Sigma-Aldrich) for 10 minutes. Samples were rinsed and differentiation was completed in borax-ferricyanide solution for 4 minutes. Tissues were dehydrated through 70%, 95%, and 100% ethanol then cleared with Histo-Clear (National Diagnostics). Images were acquired using Leica DM5500B microscope and processed in Photoshop.

Electron microscopy

Blocks containing spinal cord lesions were sectioned using a UC7 Leica Microsystems ultramicrotome (z=120 nm). Ultrathin sections were placed in silicon wafers, and carbon taped in aluminum stubs for high-resolution scanning electron microscope (SEM) imaging in a Helios NanoLab 660 FIBSEM (ThermoFisher). To maximize the collection of the backscattered electrons, a concentric detector in immersion mode was used at a 4 μm working distance, using 2 kV and 0.40 nA current landing. Overviews of the entire spinal cord were performed in low magnification (1000x) to identify all lesioned and peri-lesioned areas, then high-resolution tile images of neurovascular units in lesioned and peri-lesioned areas were performed using 35,000x magnification (5 ms, 3072x2048 resolution) with a pixel size of 3.8542 nm (MAPS 3.17, ThermoFisher).

RNA sequencing

Total RNA was extracted using the RNeasy Plus Micro Kit (Qiagen) according to the manufacturer's protocol. Two spinal cords were combined to isolate sufficient RNA for sequencing. RNA was sequenced at Q^2 Solutions Genomics (North Carolina, USA) using NovaSeq-Sequencing-2x50bp-PE on an Illumina sequencing platform. Illumina TruSeq Total RNA sample preparation kit (Illumina) was used to generate the cDNA library, and final libraries were normalized and pooled. The median number of reads across all samples was 61.4 million with 51.7 million reads after removal of sequencing artifacts. Quality checks were performed before and after FASTQ creation, including assessment of RNA quantity and integrity. Residual Illumina adapter sequences and low-quality bases from ends of reads were removed. PhiX spike-ins were used as controls, and off-target biological material percentages were measured. After removing technical and control sequences, read depths were 52.9 to 74.3 million with a median of 61.4 million. Following sequencing, samples were analyzed with the Q^2 RNAv10 pipeline. Gene and Isoform Quantification was performed. Samples were aligned using STAR gapped-read aligner (version 2.6.1d) and quantified using RSEM (version 1.3.1). Following alignment, 91.5% of reads were aligned to the transcriptome or genome. Limma-Voom package was utilized to perform differential gene expression analysis [22]. Pathway analysis was performed with Ingenuity Pathway Analysis (QIAGEN) using p-values and log fold changes of each gene found to be differentially expressed by Limma-Voom differential gene expression analysis. Statistical significance was set at $p<0.05$.

Quantification of blood vessel area and cell density around blood vessels

Using EM images, area of blood vessels within lesions was measured in Fiji. After setting the scale, the freehand shape tool was used to trace the blood vessel and total area was measured. In healthy controls, images of blood vessels were taken from the ventral portion of the spinal cord. Four to nine blood vessels were analyzed in each group (healthy control, EAE control, and B cell depleted EAE).

To measure cell densities around blood vessels in toluidine blue stained semi-thin sections, 40x images of 3-5 lesion areas were taken from 1-2 sections of the thoracic spinal cord of 3-4 animals in each group. Using the freehand shape tool in Fiji, blood vessels were traced and the number of cells within a 50 μm radius from the perimeter of each blood vessel counted. The number of cells was divided by the blood vessel region of interest (ROI) within each 40x image to determine cell density where the blood vessel ROI was defined as the area within a 50 μm radius from the perimeter of the blood vessel with the area of the blood vessel subtracted.

Measurement of area of immunostaining and white matter area

Single cells and areas of immunostaining were counted and measured with Fiji software. To measure the area of white matter, the freehand shape tool was used to outline spinal cord white matter and the total GFAP expression in white matter calculated by calculating the percent area within the outlined white matter that was labeled.

Statistical analysis

Statistical analysis was performed with GraphPad Prism 9 with statistical significance set at $p<0.05$. Student's two-tailed unpaired *t* tests were used to compare two groups. Data are presented as the mean ± SD. In addition to RNA sequencing analysis performed above, further pathway and differential gene expression analysis was performed using Ingenuity Pathway Analysis (QIAGEN) and Gene Ontology Enrichment Analysis (geneontology.org) with statistical significance set at $p<0.05$. Heat maps were generated with GraphPad Prism 9.

RESULTS

Anti-CD19/anti-B220 reduces disease severity and myelin damage in EAE

To determine the effects of B cell depletion on myelin damage and disease severity, 12-16 week-old female WT animals were induced with EAE, and peripheral B cell depletion was initiated by anti-CD19/anti-B220 administration i.p. when the animals reached a clinical score of 2.5 (limp tail and dragging of hind legs or no movement in one leg) approximately 5 days after symptom onset. Control animals received equivalent volume of IgG2a antibody. Animals were treated every 3 days for a total of 5 doses (20 days after symptom onset) and the efficacy and duration of B cell depletion in the periphery assayed. B cells (B220+) were quantified in the spleen by immunofluorescence (Fig. 1A). Compared to control EAE animals, B cell depleted animals showed an 85% reduction in the number of B220+ B cells in the spleen. The depletion of B cells was relatively uniform throughout the spleen, and the remaining cells were uniformly distributed in white pulp regions.

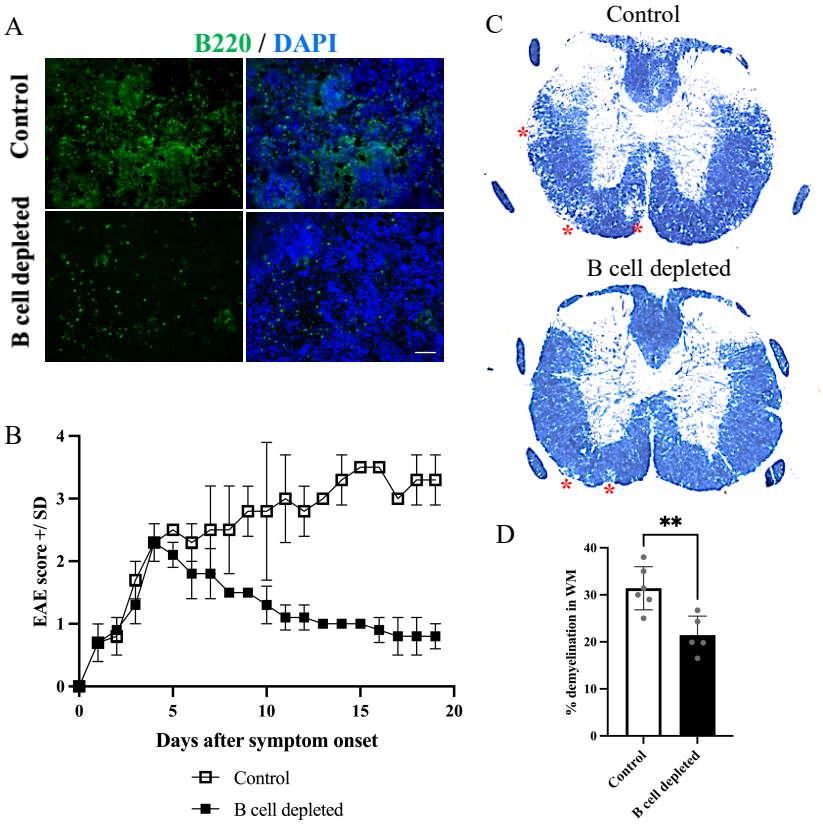


Fig. 1 B cell depletion reduces disease severity in EAE. A) Representative IHC of the spleen from control and B cell depleted EAE animals. B) Clinical scores of control EAE and B cell depleted EAE animals. C) Representative Eriochrome cyanine-R staining and D) quantification of control EAE and B cell depleted EAE spinal cords. Red asterisks indicate lesions. Scale bar = 50 μm. Data represent the mean ± SD. **$p<0.01$; compared with the corresponding controls, in 5-6 animals (Student's *t* test).

B cell depletion resulted in a rapid reversal of functional deficits in EAE. While control animals showed a steady worsening of symptoms and increase in clinical score with an average score of 3.7 at 20 days after symptom onset, B cell depleted animals showed a steady improvement and decrease in clinical score that was evident rapidly following treatment resulting in an average score of 1.0 at 20 days after symptom onset (Fig. 1B). The reduction in functional score was detectable 1-2 days after B cell depletion and was significantly different from controls 3 days following treatment ($p=0.04$) and continued to diverge for 15 days. Pathological changes in EAE are most pronounced in the spinal cord, and to determine whether changes in functional behavior correlated with alterations in the extent of spinal cord lesions, myelin damage was assayed in the thoracic spinal cord by Eriochrome cyanine R staining at 20 days post symptom onset. Quantitative analysis showed reduced levels of myelin damage and fewer lesions after B cell depletion compared to control animals (Fig. 1C). For example, while the degree of demyelination was 31.4% of total white matter area in EAE controls, in comparable spinal cord sections of B cell depleted animals, it was significantly reduced at 21.4% ($p=0.0041$; Fig. 1D). These data suggest that depletion of peripheral B cells during acute disease improves functional outcomes and reduces the extent of spinal cord myelin damage in EAE.

B cell depletion reduces microglia and astrocyte reactivity

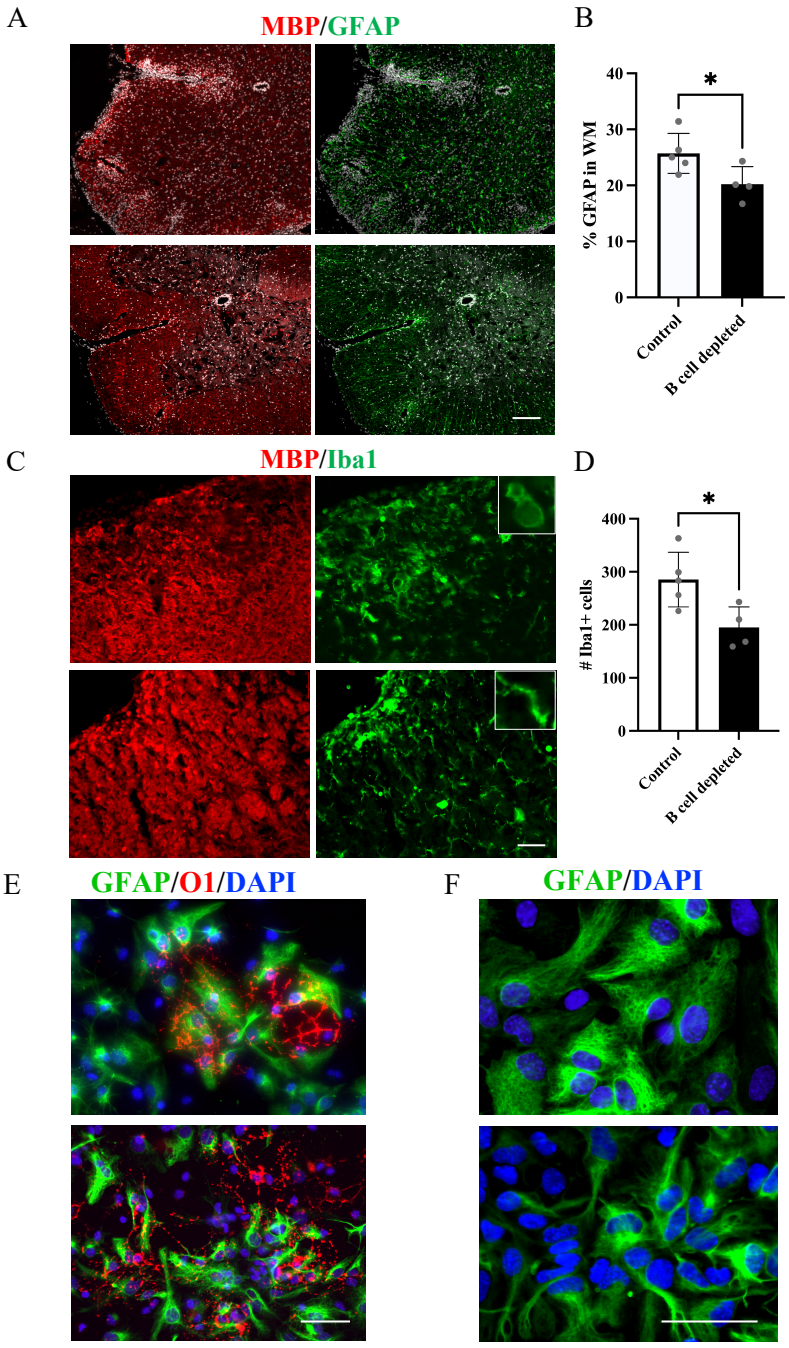


Fig. 2 B cell depletion in EAE reduces astrocyte and microglia reactivity. A) Representative IHC of GFAP+ astrocytes in a demyelinated lesion of the spinal cord and B) quantification of GFAP expression in the white matter showing reduced GFAP expression in B cell depleted spinal cord. C) Representative IHC of Iba1+ microglia/macrophages in the lesion of the spinal cord and D) quantification of the number of Iba1+ cells within the white matter per 10 µm section. B cell depletion resulted in markedly reduced size of cell bodies and increased length of processes and number of cells. E) Representative IHC of GFAP+ astrocytes and O1+ oligodendrocytes co-cultured with healthy or EAE B cells showing fragmented O1 staining with EAE B cells. F) Representative IHC of GFAP+ astrocytes alone co-cultured with healthy or EAE B cells showing shorter, denser processes in astrocytes co-cultured with EAE B cells. The insets indicate regions of high magnification. Data represent the mean ± SD. *p<0.05; compared with the corresponding control, in 5-6 animals (Student's *t* test). Scale bars = 50 µm.

Microglia and astrocyte reactivity have been implicated in neurotoxicity and disease pathogenesis in EAE [23,24]. However, it is unclear if in EAE, B cells contribute to promoting toxic glial reactivity. To address this issue, microglia and astrocyte morphology and expression of inflammatory and activation markers were analyzed by immunofluorescent staining 20 days after symptom onset. One characteristic of reactive astrocytes is the increased expression of the intermediate filament protein GFAP [25]. Quantification of GFAP expression showed significantly reduced astrocyte GFAP immunostaining in spinal cord white matter in B cell depleted EAE animals (20%) compared to EAE controls (26%; p=0.04), suggesting decreased astrocyte reactivity (Fig. 2A, B). In addition, qualitative assessment of immunostaining with Iba1 revealed morphological changes in microglia/macrophages, notably reduced cell body size and increased length of processes, indicating less microglial reactivity after B cell depletion in EAE (Fig. 2C). The number of Iba1+ cells in the spinal cord was also significantly decreased after B cell depletion (p=0.02), possibly reflecting fewer CNS infiltrating macrophages (Fig. 2D), suggesting that the reduction in functional deficits seen following B cell depletion in EAE may reflect a role for B cells in promoting chronic glial reactivity within the spinal cord. To determine whether B cells in EAE promote oligodendrocyte damage in the presence of astrocytes, glial cells isolated from healthy neonatal animals were differentiated into oligodendrocytes and astrocytes then co-cultured with healthy or EAE splenic B cells. Mixed glial cultures with oligodendrocytes and astrocytes co-cultured with EAE B cells showed significant loss of oligodendrocytes as shown by fragmented O1 immunostaining (Fig. 2E), suggesting that EAE B cells promote oligodendrocyte damage. In the *in vitro* conditions used, oligodendrocytes are dependent on astrocytes for survival. Co-culture of EAE B cells with astrocytes alone resulted in morphological changes, specifically from a more fibroblastic flattened phenotype to shorter, denser processes (Fig. 2F). Although morphology of cells *in vivo* cannot be exactly replicated *in vitro*, these data suggest that B cells in EAE directly target astrocytes. These results support the notion that B cells and/or their products in EAE infiltrate the CNS and influence astrocytes, resulting in injury or loss of oligodendrocytes and myelin.

B cell depletion results in increased blood brain barrier integrity

The functional and morphological changes in glial cells following B cell depletion may reflect either a direct effect of B cells on glial neuroinflammatory pathways or an indirect effect resulting from perturbation of CNS vascular integrity. Previous studies have shown a disruption of BBB integrity in EAE [2,26,27], and to determine whether the depletion of B cells affects BBB integrity and leakage, the expression of the tight junctional protein claudin 5 and the extent of albumin leakage were compared between control EAE and B cell depleted animals 20 days after symptom onset. Histological analysis of BBB integrity revealed disruption of claudin 5 around blood vessels in the EAE spinal cord (Fig. 3A). While in control spinal cord, the expression of claudin 5 was relatively uniform around the

vessels, in EAE tissue, claudin 5 expression was fragmented. Following B cell depletion, the disruption was less apparent, and the expression of claudin 5 was more uniformly localized, suggesting greater integrity of the blood brain barrier (Fig. 3A).

Perturbations to the BBB result in elevated entry of peripherally-derived immune cells as well as the leakage of serum proteins, such as albumin, into the spinal cord parenchyma. To compare the levels of BBB leakage between EAE and B cell depleted spinal cord samples, albumin leakage was evaluated. Extravasation of serum albumin was reduced in B cell depleted EAE animals compared to EAE controls (Fig. 3B). While in control EAE spinal cords, the spread of albumin immunoreactivity was extensive and extended up to 90 µm from the vessel's edge, in B cell depleted samples, there was limited spread of albumin into the spinal cord parenchyma. These observations suggest that B cell depleting treatment improves blood vessel junctional integrity and enhances BBB function in chronic EAE, preventing entry of serum proteins.

Astrocyte and microglia/macrophage transcriptional responses in EAE

Previous studies have highlighted the roles of astrocytes in neuroinflammation and BBB function [28–31]. Since EAE and subsequent B cell depletion influence glial reactivity and BBB function, astrocyte and microglia responses to EAE were interrogated by cell type specific RNA sequencing during acute disease. To assess acute EAE-induced changes in astrocyte gene expression, ACSA2+ purified astrocytes were isolated from the spinal cord 3 days after animals reached a clinical score of 2.5 during the acute phase of EAE. Previous studies have demonstrated the utility of ACSA-2 as a specific marker for astrocytes in the adult murine CNS and its effectiveness for cell isolation [32,33]. Cell type specific RNA sequencing and comparison of EAE astrocytes and non-EAE control astrocytes by gene ontology (GO) enrichment analysis revealed inflammation-associated biological processes and molecular functions as the top GO terms in astrocytes (Fig. 4A-C). Specifically, genes associated with astrocyte mediated inflammation were found to be over-represented in EAE astrocytes compared to non-EAE control astrocytes. The top differentially expressed biological processes include neutrophil degranulation (gene count = 234) and signaling by interleukins (gene count = 198; Fig. 4A) where the gene count represents the number of genes associated with the GO term. Top molecular functions include terms such as pattern recognition receptor activity, cytokine receptor activity, immune receptor activity, and cytokine binding (fold enrichment = 2.83, 2.26, 2.2, 1.95, respectively; Fig. 4B). Furthermore, genes involved in platelet activation were enriched in EAE astrocytes compared to non-EAE animals (gene count = 116). Platelet activation is an early process in EAE pathogenesis, promoting inflammation and recruitment of leukocytes to the CNS [34], and astrocytes have been shown to activate platelets by secreting factors such as TNFα [35]. To identify potential signaling pathways influenced by B cell depletion in EAE, Ingenuity Pathway Analysis (IPA) was performed on spinal cord astrocytes. Comparison of the

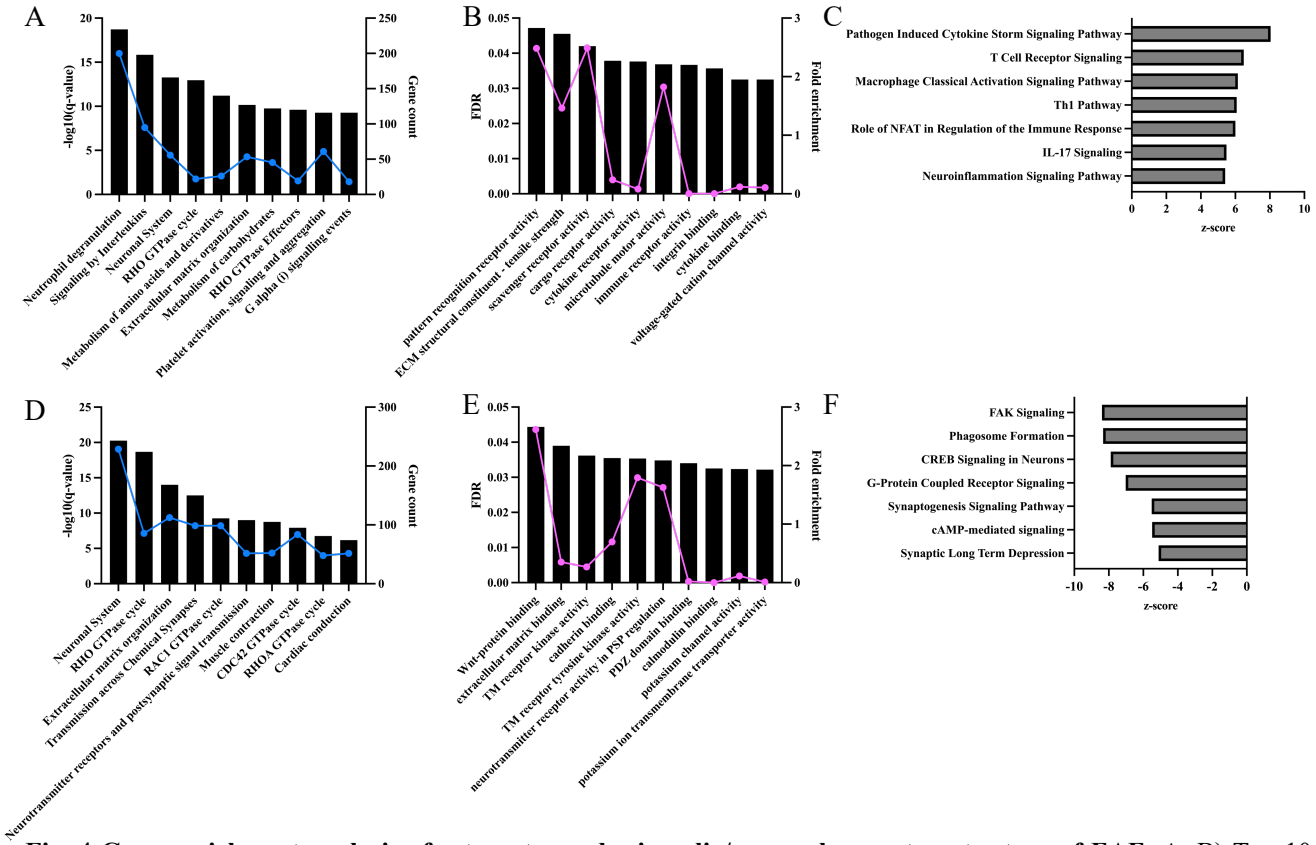


Fig. 4 Gene enrichment analysis of astrocytes and microglia/macrophages at acute stage of EAE. A, B) Top 10 enriched GO terms and C) top canonical pathways by Ingenuity Pathway Analysis of spinal cord astrocytes from EAE animals, normalized against healthy controls. D, E) Top 10 enriched GO terms and F) top canonical pathways by Ingenuity Pathway Analysis of spinal cord microglia from EAE animals, normalized against healthy controls. A, D) Bars show gene counts and lines show -log10(q-value) of top 10 biological processes. Q-values are FDR-adjusted p-values or the minimum FDR at which values are deemed significant. B, E) Bars show fold enrichment and lines show FDR of top 10 molecular functions. FDR is the rate that significant features are found to be truly null. FDR $p<0.05$.

top upregulated pathways in EAE versus healthy control were related to immune activation, including pathogen induced cytokine storm, T cell receptor signaling, Th1 pathway, MS signaling, and neuroinflammation signaling (Fig. 4C). Taken together, these data support pronounced inflammatory activity and structural changes in spinal cord astrocytes during acute EAE.

A similar approach was used to assess gene changes in CD11b+ purified microglia/macrophages in response to acute EAE. CD11b+ cells were isolated from the spinal cord during the acute phase of EAE when animals reached a clinical score of 2.5-3, and transcriptional differences compared between cells from EAE and healthy control animals. GO enrichment analysis revealed changes in extracellular matrix organization, transmission across chemical synapses, and postsynaptic signal transmission to be the top biological processes (gene count = 168, 150, 108, respectively; Fig. 4D), highlighting the role of microglia in synapse degeneration and neuronal function. Molecular functions elevated in EAE CD11b+ cells include Wnt-protein binding, ECM binding, and transmembrane receptor kinase activity (fold enrichment = 2.66, 2.34, 2.17; Fig. 4E). Notably, genes involved in ECM processes were found to be highly enriched in microglia/macrophages. Such changes may reflect microglial reactivity that include changes in cell structure, including size and shape of cell bodies and processes. Furthermore, IPA of spinal cord CD11b+ cells revealed that EAE induction downregulates genes associated with several pathways including cAMP response element-binding protein (CREB) signaling in neurons, FAK signaling, phagosome formation, synaptogenesis signaling, and signaling of Rho family GTPases (Fig. 4F), confirming GO analyses. These findings highlight the importance of microglia in modulating neuronal activity in EAE progression. Altogether, these data reveal that EAE induces specific changes in astrocyte and microglia gene expression that implicate their role in CNS injury.

Astrocytes and microglia/macrophages responses after B cell depletion

The finding that B cell depletion reduces functional deficits, spinal cord damage, and glial reactivity in EAE suggests that glial transcriptional changes induced by EAE may be modulated by B cell depletion. To identify potential pathways modulated by B cells, EAE animals were treated with a single dose of anti-CD19/anti-B220 when animals reached a clinical score of 2.5. The transcriptomes of purified EAE spinal cord astrocytes and microglia were then compared with transcriptomes of EAE glia 3 days after B cell depletion to identify gene expression changes acutely associated with B cell loss. While there were 5534 differentially expressed genes between ACSA2+ astrocytes isolated from EAE and healthy control animals and 3272 differentially expressed genes between B cell depleted EAE and healthy control animals, only 57 differentially expressed astrocyte genes were detected between EAE and B cell depleted EAE animals (Table 1). Similarly, there were 7379 differentially expressed genes in CD11b+ cells isolated from EAE versus healthy control animals and 4561 differentially expressed genes in B cell depleted EAE versus healthy control animals but only 319 differentially expressed genes were detected in CD11b+ cells from B cell depleted versus control EAE animals. This suggests that while B cell depletion has a profound rapid effect on the functional outcome of disease, it initially targets relatively few genes in astrocytes and microglia.

Table 1 Number of differentially expressed genes in astrocytes and microglia

Comparison	Reference Group	Comparator Group	(1) Num Sig. Adj. P<0.05	(2) (1)+|L2FC|>0.25	(3) (2)+Homologous
1	Astrocytes Untreated EAE	Astrocytes Treated EAE	64	64	57
2	Astrocytes Healthy Controls	Astrocytes Treated EAE	4925	4925	3272
3	Astrocytes Healthy Controls	Astrocytes Untreated EAE	8150	8150	5534
4	Microglia Untreated EAE	Microglia Treated EAE	367	367	319
5	Microglia Healthy Controls	Microglia Treated EAE	6132	6132	4561
6	Microglia Healthy Controls	Microglia Untreated EAE	10578	10578	7379

In astrocytes, the top significantly downregulated genes in B cell depleted compared to control EAE animals were *CHIA, COL20A1, MOXD1, SIGLEC1*, and *KIFC1* (Fig. 5A). These genes were upregulated in EAE compared to healthy controls, suggesting that the expression of these genes is reversed as a result of B cell loss. Specifically, *CHIA* mediates IL-13 function in inflammation [36], and *SIGLEC1* is a cell adhesion molecule that is upregulated during inflammation [37]. While the exact role of these genes in MS are unknown, these data indicate that genes associated with inflammation in astrocytes are upregulated during EAE progression and downregulated after B cell depletion. However, GO and IPA analyses revealed that neuroinflammatory pathways are not reversed after B cell depletion (Fig. 5B). Unexpectedly, the majority of the pathways that were predicted to be activated during EAE progression were not reversed 3 days following B cell loss even though there was functional recovery. Rather, the top differentially expressed pathways in B cell depleted compared to control EAE astrocytes where focal adhesion kinase (FAK) signaling and neurovascular coupling signaling, both of which were predicted to be activated. These data are consistent with the hypothesis that functional recovery after B cell depletion is initiated through improvements in the neurovasculature rather than suppression of inflammatory responses.

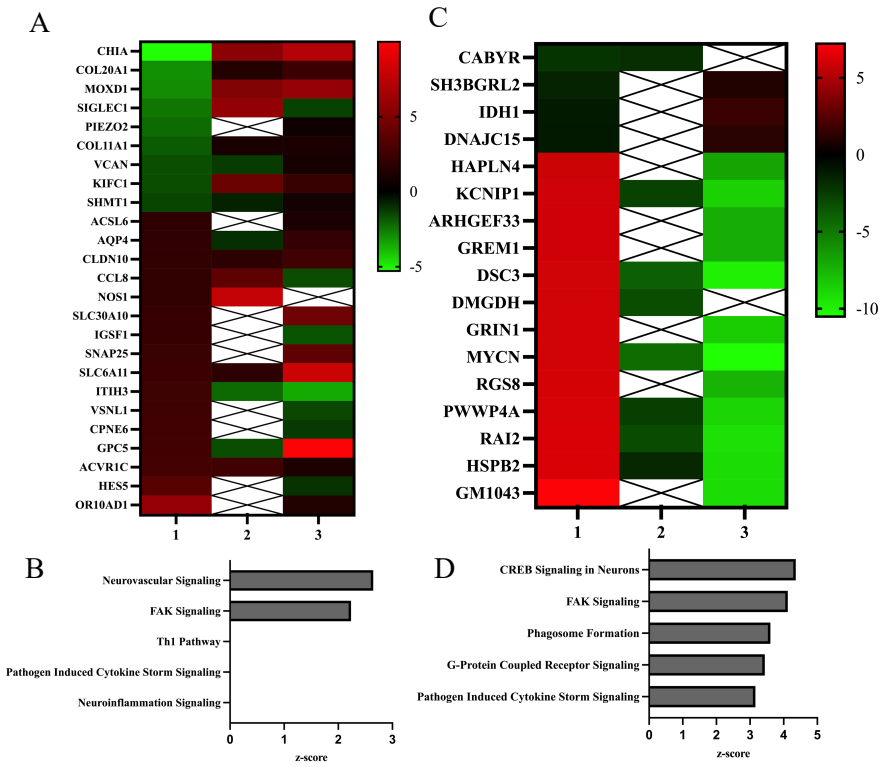


Fig. 5 Differentially expressed genes and canonical pathways in spinal cord astrocytes and microglia/macrophages after B cell depletion. A) Top differentially expressed genes in astrocytes isolated from B cell depleted EAE versus control EAE animals (column 1) and corresponding fold changes in astrocytes isolated from B cell depleted EAE versus healthy controls (column 2) and control EAE versus healthy controls (column 3). B) Canonical pathways for astrocytes of B cell depleted EAE versus control EAE animals showing neurovascular and FAK signaling pathways to be activated and no differences in immune related pathways. C) Top differentially expressed genes in microglia/macrophages isolated from B cell depleted EAE versus control EAE animals (column 1) and corresponding fold changes in microglia/macrophages isolated from B cell depleted EAE versus healthy controls (column 2) and control EAE versus healthy controls (column 3). D) Top canonical pathways in microglia/macrophages of B cell depleted EAE versus control EAE animals showing predicted activation of CREB signaling in neurons and GPCR signaling.

In microglia/macrophages isolated from B cell depleted compared to EAE animals, genes involved in neuronal activity such as *Cabyr* and *Sh3bgrl2* were found to be downregulated (Fig. 5C. Although *Cabyr* was downregulated in CD11b+ cells from B cell depleted EAE compared to control EAE samples, it was not significantly upregulated in EAE cells over healthy controls, suggesting it may be inhibited as a result of B cell depletion but does not play a significant role during EAE progression. Somewhat unexpectedly, all of the top upregulated genes in CD11b+ cells from B cell depleted EAE compared to control EAE animals were significantly downregulated in CD11b+ cells from EAE compared to healthy controls. Of note were *Rgs8,* which is involved in scaffolding of G-protein gated ion channels [38], *Grin1*, a glutamate receptor [39], and *Grem1,* which inhibits monocyte migration and activates STAT3 signaling [40]. Expectedly, pathway analysis revealed a similar reversal of transcriptional responses. While microglia-neuron communication in synaptogenesis, CREB signaling, and synaptic transmission, for example, were found to be inhibited in EAE (Fig. 4), following B cell depletion, the top canonical pathways were all predicted to be activated, including CREB and GPCR signaling in neurons (Fig. 5D). Previously, it has been shown that enhanced CREB signal transduction suppresses pro-inflammatory microglial responses [41], suggesting that a loss of B cells in EAE reverses pro-inflammatory functions in microglia. Additionally, GPCRs have been studied as therapeutic targets in neuroinflammatory diseases because of their ability to inhibit microglial activation and modulate inflammation [42]. Taken together, these findings suggest that many of the changes in gene expression induced by EAE in CD11b+ cells are quickly reversed after B cell depletion, and these targets modulate neuronal function.

Together, the astrocyte and microglial responses immediately following B cell depletion indicate that inhibition of pro-inflammatory pathways in EAE may be a secondary response and that the primary driver of functional recovery is improvement in neurovascular integrity and neuronal function.

B cell depletion activates FAK and Neurovascular Coupling Signaling Pathways in Astrocytes

A detailed analysis of the genes involved in the neurovascular coupling pathway showed several upregulated genes after B cell depletion, including genes associated with inflammation (*NOS1*) and neuronal and neurotransmitter activity (*GABBR2, GRIA1, SLC1A2,* and *GABRG1*; Fig. 6A). Of these genes, *GABBR2, SLC1A2, ABHD3, and GABRG1* were also downregulated in EAE versus healthy control animals. Following B cell depletion, significantly upregulated astrocyte genes in the FAK signaling pathway include genes associated with TGFβ signaling (*ACVR1C),* neuronal activity (*GABBR2*) and cell migration (*SPARCL1*) (Fig. 6B). Of these genes, *ACVR1C* and *GABBR2* were downregulated in EAE microglia compared to healthy controls. Notably, most of the genes involved in FAK signaling were downregulated in EAE versus healthy control animals but significantly upregulated after B cell depletion. FAK signaling directs numerous signal transduction pathways. For example, in astrocytes, FAK has been shown to regulate astrocyte morphology as well as proliferation [43,44]. The FAK pathway was, however, also upregulated in EAE compared to healthy controls, suggesting this pathway is activated as a result of changes in general astrocyte function and not specifically related to B cell depletion. By contrast, neurovascular coupling was downregulated in control EAE animals compared to controls and reversed by B cell depletion suggesting B cell depletion may influence vasculature integrity and affect peripheral cell infiltration. These data suggest that the mechanisms that promote disease in EAE are not necessarily the same mechanisms that reverse disease as an immediate response to B cell depletion.

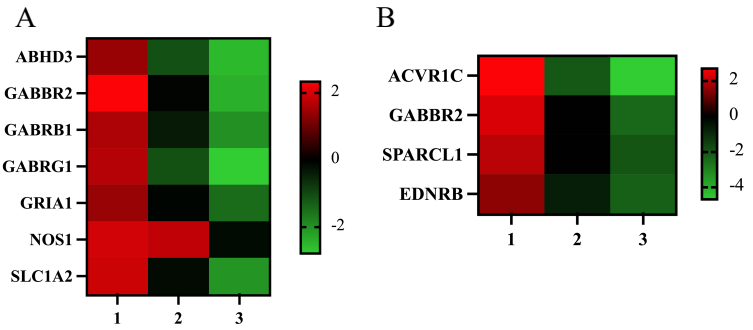


Fig. 6 Expression of genes involved in neurovascular coupling and FAK signaling in astrocytes. A) Top differentially expressed genes in the neurovascular coupling signaling pathway reveal NOS1 and GRIA1 as significantly upregulated in B cell depleted compared to control astrocytes. While GABBR2, SLC1A2, ABHD3, and GABRG1 were significantly downregulated in control EAE versus control healthy animals, they were upregulated in B cell depleted EAE versus control EAE animals. B) Top differentially expressed genes in the FAK signaling pathway reveal SPARCL1 as significantly upregulated in B cell depleted EAE versus control EAE astrocytes. ACVR1C, GABBR2, and EDNRB were significantly downregulated in EAE versus healthy animals while they were significantly upregulated in B cell depleted EAE versus control EAE animals. Column 1 represents differentially expressed genes in astrocytes isolated from B cell depleted EAE versus control EAE animals. Column 2 represents B cell depleted EAE versus healthy controls. Column 3 represents control EAE versus healthy controls.

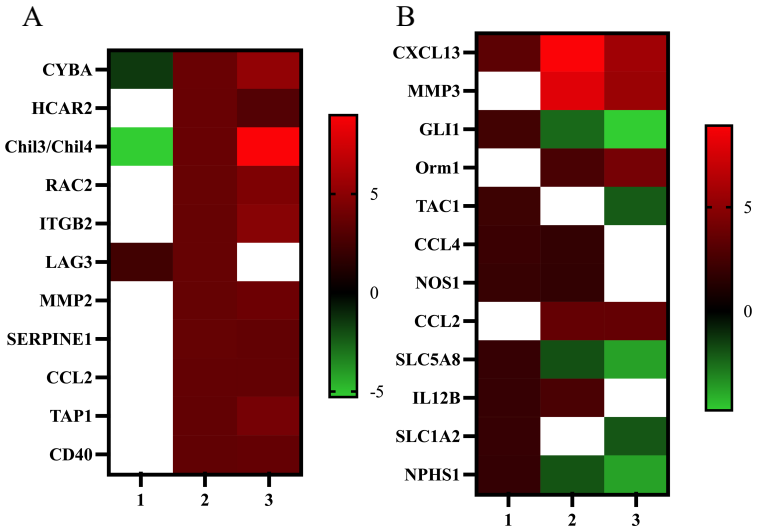


Fig. 7 Top differentially expressed genes in neuroinflammatory signaling pathways. A) Top differentially expressed genes in IFNγ signaling reveals Chil3/Chil4 is significantly downregulated in astrocytes isolated from B cell depleted EAE compared to control EAE animals. B) Top differentially expressed genes in TNFα signaling reveals NOS1 and CCL2 are significantly upregulated compared to control EAE animals. SLC1A2 is downregulated in EAE versus healthy animals but upregulated in astrocytes isolated from B cell depleted EAE compared to control EAE animals. Column 1 represents differentially expressed genes in astrocytes isolated from B cell depleted EAE versus control EAE animals. Column 2 represents B cell depleted EAE versus healthy controls. Column 3 represents control EAE versus healthy controls.

Genes in neuroinflammatory pathways are differentially expressed after B cell depletion

As outlined above, the pathways most affected by EAE induction are largely immune related (Fig. 4). While IPA did not reveal these pathways to be differentially activated after B cell depletion, further analysis into the specific genes involved in inflammatory signaling pathways revealed moderate differences. In the IFNγ signaling pathway, *Chil3/Chil4* was found to be significantly downregulated after B cell depletion whereas in EAE, it was significantly upregulated compared to healthy controls (Fig. 7A). *Chil3/Chil4* along with other chitin family genes, including *CHI3L1* and *CHI3L2,* are elevated in astrocytes in neuroinflammatory diseases such as MS and may contribute to inflammation by activating mitogen-activated protein kinase (MAPK) signaling pathways [36,45–47]. Furthermore, in the tumor necrosis factor alpha (TNFα) signaling pathway, *NOS1, CCL2,* and *SLC1A2* were found to be downregulated after B cell depletion (Fig. 7B) compared to control EAE. *SLC1A2* is a glutamate transporter and not typically associated with cytokines but is downregulated by TNFα [48], and EAE is characterized by high levels of TNFα production in the CNS [49,50]. Remarkably, the current data indicates that while *SLC1A2* was downregulated after B cell depletion, it was upregulated in EAE animals compared to controls. This suggests that while high TNFα downregulates *SLC1A2*, other mechanisms involved in EAE progression may upregulate *SLC1A2* expression in astrocytes. Overall, these results reveal the complexity of inflammatory signaling and confirm that the signaling pathways that drive disease may not be the ones that are immediately reversed after B cell depletion.

BBB impairment is reduced as a result of B cell depletion

Astrocytes are crucial for the integrity of the BBB and neurovascular unit and contribute to the cerebral vasculature [51,52]. Loss of astrocytic endfeet, common in diseases such as MS, is accompanied by BBB impairment and inflammation [53–55]. As vasodilation is a significant aspect of inflammation [55], blood vessel area in the EAE spinal cord was measured. Compared to healthy controls, blood vessels in the spinal cord were dilated as indicated by the increase in the range of blood vessel area, the largest blood vessel measuring 4240 μm^2 compared to 413 μm^2 in healthy controls (Fig. 8A). Following B cell depletion, significantly dilated blood vessels were no longer observed, the largest vessel measuring 169 μm^2. As astrocyte endfeet make close contact with blood vessels and release signals that contract and dilate vessels [56–58], endfeet coverage of blood vessels was examined. Dilation of blood vessels was accompanied by a loss of astrocyte endfeet coverage around the blood vessels (Fig. 8B). In control EAE animals, there was a profound loss of astrocyte foot processes ensheathing blood vessel endothelial cells. After B cell depletion, endfeet coverage was recovered, suggesting that a loss of B cells restores astrocyte function that may contribute to restoration of BBB integrity. Disruptions of the BBB in the setting of EAE and MS leads to a high influx of peripheral immune cells into the spinal cord, which may directly contribute to glial reactivity and inflammation.

Transcriptional analysis of spinal cord astrocytes revealed changes in genes associated with the neurovascular unit in EAE that were reversed following B cell depletion. To determine if such changes influenced immune cell infiltration, toluidine blue semi-thin sections

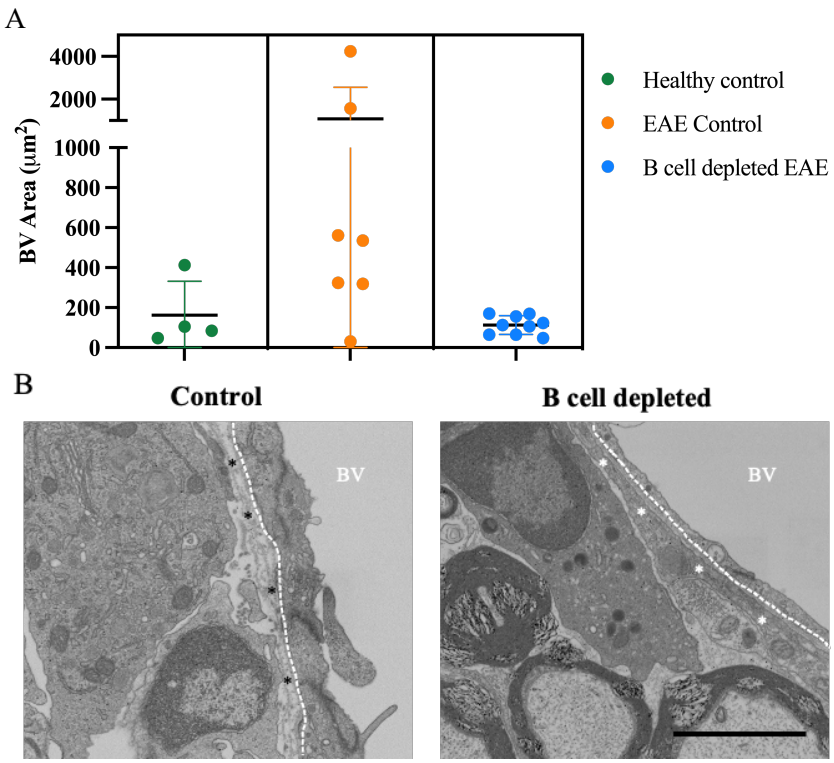


Fig. 8 EAE is characterized by blood vessel dilation and compromised blood vessel integrity which are reversed with B cell depletion. A) The range in blood vessel area is increased in EAE and restored after B cell depletion. Black horizontal bars indicate mean for each group. B) Electron microscopic observations of blood vessels in the EAE spinal cord reveal a loss of coverage of endothelial cells by astrocyte endfeet and restoration of coverage after B cell depletion. White dashed line outlines the endothelial cells. Black asterisks and white asterisks indicate loss of and presence of astrocyte endfeet, respectively. Scale bar = 2 µm. BV = Blood vessel.

of control EAE and B cell depleted EAE thoracic spinal cords were analyzed for cell infiltration around blood vessels within demyelinated white matter lesions. Vessels in spinal cord lesion areas of EAE animals were characterized by a halo of infiltrating cells that was significantly reduced in cell number and area in B cell depleted EAE animals ($p=0.02$; Fig. 9). The reduction in cell infiltration is consistent with the data from analysis of astrocyte transcriptomes showing downregulation of neurovasculature genes in EAE and their upregulation following B cell depletion (Fig. 6A). Dysfunction in neurovascular coupling is often correlated with dysfunction of the BBB [59], suggesting that improved BBB function may be responsible for the reduced cell infiltration in B cell depleted EAE that contributes to the functional recovery from EAE.

DISCUSSION

Currently, B cell targeted therapies are one of the most effective immunomodulatory treatments in patients with relapsing-remitting and primary progressive MS [15,16]. However, the precise mechanisms mediating functional recovery are not well defined. Using an EAE animal model that engages B cells, we demonstrated that depleting B cells during the acute phase of EAE reverses disease, and extended B cell depletion reduces astrocyte and microglia reactivity as well as myelin damage in the spinal cord. Cell specific RNA analysis identified transcriptional changes in astrocytes and microglia 3 days following B cell depletion, suggesting that B cell depletion rapidly alters the transcriptome of glial cells that likely contribute to functional recovery. Compared to healthy controls, astrocytes isolated from EAE animals showed an upregulation of immune related mechanisms, including Th1, cytokine storm, and neuroinflammation signaling pathways. Somewhat unexpectedly, the functional recovery seen following B cell depletion was not associated with a wide scale reduction in the inflammatory profile. Rather, following B cell depletion, pathways related to neurovascular coupling were upregulated, suggesting an improvement in blood vessel integrity. Consistent with an improvement in vascular integrity, following B cell depletion claudin 5 expression was relatively uniform around vessels, the leakage of albumin was significantly reduced, and the extent of immune cell filtration into the spinal cord parenchyma reduced. These results suggest that B cell modulation of astrocyte and microglia function plays a critical role in not only progression of EAE but also recovery from disease.

The reduction in functional deficits following B cell depletion is consistent with clinical data in which many patients see a decrease in relapses and number of lesions by MRI after B cell depleting treatments [15,16]. While highly successful, current B cell targeted therapies have also demonstrated adverse effects where patients develop multifocal leukoencephalopathy, detect no functional recovery, or even observe progression of disease [60–62]. Furthermore, such treatments have potential side effects that include becoming immunocompromised as current depletion strategies remove antibody-producing B cells, increasing the risk for infections. The current study supports earlier work suggesting that B cells play a critical role in demyelinating disease and that CNS cells, particularly astrocytes and microglia, may be the targets of B cells and respond to both the presence and removal of B cells. Depletion of B cells in acute EAE using an anti-CD19 antibody resulted in a reduction in clinical scores along with reduced GFAP expression in astrocytes, fewer inflammatory microglia, and fewer Iba1+ cells in the lesion. It seems likely that these responses influence disease progression since astrocyte and microglia reactivity is one of the hallmarks of both relapsing-remitting and progressive stages of MS and has been implicated in disease progression [63–66].

Changes in the morphology and reactivity of astrocytes and microglia after B cell depletion suggest that B cells may influence glial functions during disease. *In vitro*, B cells isolated from EAE animals damage oligodendrocytes in the presence of astrocytes. Additionally, EAE B cells co-cultured with astrocytes alone result in morphological changes. While the morphology of the cells may not accurately reflect conditions *in vivo*, the data strongly supports the notion that astrocytes may be a cellular target of B cells in EAE. B cells may impair normal astrocyte function, including maintaining the BBB that is reversed following B cell depletion. Indeed, in EAE, increased GFAP expression and number of inflammatory microglia in the spinal cord is accompanied by reduced tight junction protein claudin 5 expression and extensive leakage of albumin. In the non-injured CNS, astrocytic endfeet cover almost the entire

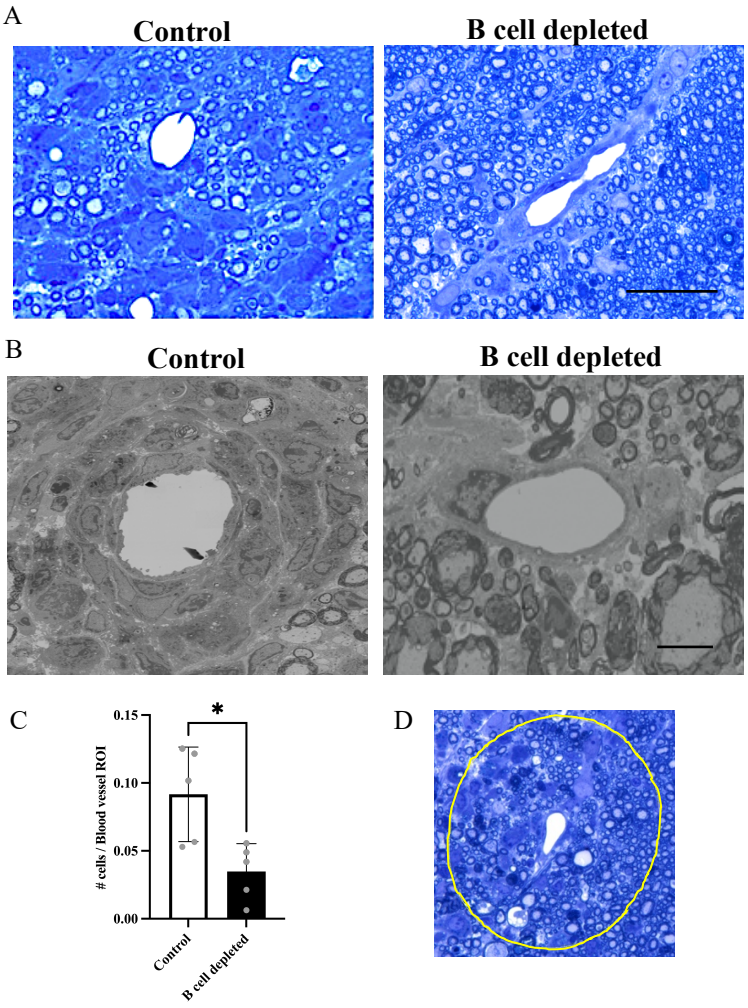


Fig. 9 Cell infiltration is reduced in spinal cords of B cell depleted EAE animals. A) Representative toluidine blue stained semi-thin sections of thoracic spinal cords of B cell depleted EAE and control EAE animals. Fewer infiltrating cells around the blood vessel are observed after B cell depletion. B) Representative SEM image of ultrathin section of thoracic spinal cords of B cell depleted EAE and control EAE animals confirm reduced cell infiltration after treatment. C) Quantification of cell infiltration measured as cell density within a demyelinated lesion in the white matter. D) Cell density is quantified by dividing the number of cells within a 50 μm radius of the perimeter of all blood vessels in a 40x image of a section of the thoracic spinal cord by the total area of the 50 μm radius subtracted by the area of the blood vessels. Each data point represents an average of the cell density of 3-5 different lesion areas in the spinal cord of one animal. n=5 animals per treatment group. *p<0.05. Scale bar = 50 μm.

vascular surface [67], contributing to the structural integrity of the BBB. Consistent with this central role for astrocytes in the neurovascular unit [51,52,68,69], increased astrocyte reactivity both contributes to and reflects disruption of the integrity and structure of the CNS vasculature.

Evaluation of astrocytes and microglia during peak disease revealed astrocyte mediated inflammation and microglia-neuron interactions drive disease progression in EAE. The current data reveal immune related molecular functions in astrocytes to be significantly increased in EAE, including cytokine receptor activity and cytokine binding. In addition to inflammatory mechanisms such as astrocytic neurovascular coupling signaling is downregulated, suggesting that during this highly active stage of disease, astrocytes may promote further damage by compromising the vasculature of the CNS and permitting more immune cells into the CNS. Indeed, astrocytes secrete TNFα, IL6, and GM-CSF in EAE [70], which then propagate neuroinflammation and lead to neuronal damage. Microglial cells are highly responsive to perturbations of the CNS, and the transcriptional analysis of purified CD11b+ cells indicates that induction of EAE has profound effects on gene expression across a broad range of signaling pathways. Among the most upregulated pathways in EAE were Wnt signaling, ECM and synaptic transmission pathways that likely reflect cellular activation and the role of microglia on modulating neuronal responses. Given the role of microglia in immune responses it was surprising that pro-inflammatory signaling pathways were not more elevated in EAE. However, previous studies suggest a role for microglia in regulation of neuronal activity [71] and a study by Badimon et al., indicated microglia sense activation and inhibition of neurons and respond by extending and retracting processes and increasing and decreasing motility [71]. While the direct relationships between B cells, astrocytes, and microglia remain unclear, these data suggest that B cells during disease impair astrocyte function in the CNS, weakening the BBB and propagating inflammation. Consequently, inflammatory microglia reduce normal neuronal modulatory activity consistent with a prominent role for modulation of glial activity in mediating disease progression.

The proinflammatory and neurotoxic effects of microglia and astrocytes during acute EAE is well documented, but it is less well understood how B cell depletion treatments, such as rituximab and ocrelizumab, reverse these effects. We report here that removal of B cells downregulates pathways that are activated during acute EAE. Specifically, IPA revealed neurovascular coupling signaling in astrocytes is downregulated in control EAE and upregulated after B cell depletion. Similarly, genes associated with synaptogenesis were downregulated in EAE compared to healthy controls, and were upregulated with B cell depletion, suggesting astrocytes may play a role in neural repair. While relatively few genes were differentially expressed in astrocytes after B cell depletion, many more pathways were reversed in microglia. These findings are intriguing as astrocyte reactivity is known to persist through different stages of disease

whereas microglia may be more sensitive and responsive [72,73], which may explain why fewer transcriptional changes were found in astrocytes compared to microglia after B cell depletion.

Following B cell depletion in EAE, rapid changes to the vasculature were seen, including reduction of blood vessel area, which was dramatically increased during disease, and increased astrocyte endfeet coverage. This resulted in a dramatic reduction in CNS infiltrating cells, likely reducing inflammation. Improvement in CNS vasculature coincided with a reversal of microglial pathways upregulated during disease, implying that during disease, improved blood vessel integrity by astrocytes alters the inflammatory microglia profile. These observations are consistent with studies in MS patients treated with rituximab where there is a reduction in the number of Gadolinium enhancing lesions in the brain, suggesting recovery of blood-brain barrier function as the Gadolinium-DTPA contrast agent is not able to cross an intact blood-brain barrier [15]. Our studies suggest that one of the primary effects of B cell depletion is to promote neurovasculature function, thus reducing permeability and limiting the influx of neurotoxic peripheral components.

In MS, several abnormalities in B cell function have been identified, including cytokine dysregulation and secretion of cytotoxic and neurotoxic products [14,74,75]. These mechanisms are unrelated to antibody production, suggesting that B cells may contribute to disease through antibody-independent mechanisms. For example, Lisak and colleagues demonstrated that B cell secreted factors from relapsing-remitting MS patients induced neuronal death, microglial enlargement, and oligodendrocyte death [74,75]. While the identities of these B cell products have yet to be identified, it seems likely B cells contribute to demyelination, whether directly or indirectly through microglia and astrocytes resulting in MS pathogenesis. To our knowledge, this is the first report to show transcriptional changes in microglia and astrocytes immediately after B cell depletion in EAE. While the current studies do not define the sequence of events that lead to the changes in the transcriptome of astrocytes and microglia, one hypothesis that is consistent with the current findings is that loss of integrity in the neurovascular unit in EAE is mediated in part through B cell induced changes in astrocytes that facilitates infiltration of inflammatory cells and cytokines, which stimulate broad inflammatory responses in both astrocytes and microglia. Depletion of B cells results in the rapid recovery of vascular integrity that results in the reduction of inflammatory stimuli and subsequent functional recovery. The limited changes in astrocyte transcriptomes and the essential reversal of microglia responses following B cell depletion are consistent with this concept.

CONCLUSIONS

In summary, the current findings reveal a novel B cell-glial cell relationship in EAE and point to a mechanism by which depletion of B cells may contribute to reduction in pathology. The diversity of astrocytes and microglia with respect to morphology, function, and communication, is profound, and these studies improve our understanding of their roles in disease progression and recovery. Together, these findings enhance our knowledge of B cell and glial cell function in EAE, which may lead to identification of novel targets to selectively manipulate glial responses in MS.

ABBREVIATIONS

BBB	Blood-brain barrier
BSA	Bovine serum albumin
BV	Blood vessel
CFA	Complete Freund’s adjuvant
CNS	Central nervous system
CREB	cAMP response element-binding
DMEM	Dulbecco's modified eagle medium
DPBS	Dulbecco's phosphate-buffered saline
EAE	Experimental autoimmune encephalomyelitis
ECM	Extracellular matrix
EM	Electron microscopy
FAK	Focal adhesion kinase
FBS	Fetal bovine serum
GFAP	Glial fibrillary acidic protein
GO	Gene ontology
HBSS	Hanks' balanced salt solution
i.p.	Intraperitoneal
IFN	Interferon
IHC	Immunohistochemistry

IPA	Ingenuity pathway analysis
L2FC	Log2 fold change
MAPK	Mitogen-activated protein kinase
MBP	Myelin basic protein
MEM	Minimum essential medium
MOG	Myelin oligodendrocyte glycoprotein
MS	Multiple sclerosis
NGS	Normal goat serum
SEM	Scanning electron microscopy
TNF	Tumor necrosis factor

CRediT AUTHOR STATEMENT

Julie J. Ahn: Conceptualization, Methodology, Formal analysis, Investigation, Writing – Original Draft, Visualization, Funding acquisition. **Yusra Islam**: Investigation. **Cheryl Clarkson-Paredes**: Investigation. **Molly T. Karl**: Investigation. **Robert H. Miller**: Writing – Review & Editing, Supervision, Funding acquisition.

ACKNOWLEDGEMENTS

We thank the GW Nanofabrication and Imaging Center.

FUNDING

This work was supported by the National Institute of Neurological Disorders and Stroke [grant number F31NS117085], the U.S. Department of Defense [grant number MS210155], and the Vivian Gill Research Endowment to Dr. Robert H. Miller.

DECLARATIONS OF INTEREST

None

REFERENCES

1. Stafford, P. *et al.* Astrocytes and pericytes attenuate severely injured patient plasma mediated expression of tight junction proteins in endothelial cells. *PLoS One* **17**, e0270817 (2022).
2. Stavropoulos, F., Georgiou, E., Sargiannidou, I. & Kleopa, K. A. Dysregulation of Blood-Brain Barrier and Exacerbated Inflammatory Response in Cx47-Deficient Mice after Induction of EAE. *Pharmaceuticals* **14**, 621 (2021).
3. RV, S. *et al.* Contribution of Tissue Inflammation and Blood-Brain Barrier Disruption to Brain Softening in a Mouse Model of Multiple Sclerosis. *Front Neurosci* **15**, (2021).
4. M, A. & R, K. Comparative Review of Microglia and Monocytes in CNS Phagocytosis. *Cells* **10**, (2021).
5. Andoh, M. & Koyama, R. Comparative Review of Microglia and Monocytes in CNS Phagocytosis. *Cells* **10**, (2021).
6. Tahmasebi, F. *et al.* Effect of the CSF1R inhibitor PLX3397 on remyelination of corpus callosum in a cuprizone-induced demyelination mouse model. *J Cell Biochem* **120**, 10576–10586 (2019).
7. Nissen, J. C., Thompson, K. K., West, B. L. & Tsirka, S. E. Csf1R inhibition attenuates experimental autoimmune encephalomyelitis and promotes recovery. *Exp Neurol* **307**, 24–36 (2018).
8. D, J. *et al.* Mass Cytometry of CSF Identifies an MS-Associated B-cell Population. *Neurology(R) neuroimmunology & neuroinflammation* **8**, (2021).
9. Engel, S. *et al.* Intrathecal B-cell accumulation and axonal damage distinguish MRI-based benign from aggressive onset in MS. *Neurol Neuroimmunol Neuroinflamm* **6**, (2019).
10. NL, F. *et al.* Absence of B Cells in Brainstem and White Matter Lesions Associates With Less Severe Disease and Absence of Oligoclonal Bands in MS. *Neurology(R) neuroimmunology & neuroinflammation* **8**, (2021).
11. Brummer, T., Zipp, F. & Bittner, S. T cell-neuron interaction in inflammatory and progressive multiple sclerosis biology. *Curr Opin Neurobiol* **75**, (2022).
12. Babbe, H. *et al.* Clonal expansions of CD8 + T cells dominate the T cell infiltrate in active multiple sclerosis lesions as shown by micromanipulation and single cell polymerase chain reaction. *Journal of Experimental Medicine* **192**, 393–404 (2000).

13. Seals, M. R., Moran, M. M., Leavenworth, J. D. & Leavenworth, J. W. Contribution of Dysregulated B-Cells and IgE Antibody Responses to Multiple Sclerosis. *Front Immunol* **13**, (2022).
14. Li, R. *et al.* Proinflammatory GM-CSF-producing B cells in multiple sclerosis and B cell depletion therapy. *Sci Transl Med* **7**, (2015).
15. Hauser, S. L. *et al.* B-cell depletion with rituximab in relapsing-remitting multiple sclerosis. *N Engl J Med* **358**, 676–88 (2008).
16. Montalban, X. *et al.* Ocrelizumab versus placebo in primary progressive multiple sclerosis. *New England Journal of Medicine* **376**, 209–220 (2017).
17. Häusler, D. *et al.* Functional characterization of reappearing B cells after anti-CD20 treatment of CNS autoimmune disease. *Proc Natl Acad Sci U S A* **115**, 9773–9778 (2018).
18. Ahn, J. J., Islam, Y. & Miller, R. H. Cell type specific isolation of primary astrocytes and microglia from adult mouse spinal cord. *J Neurosci Methods* **375**, (2022).
19. Ansari, A. *et al.* An efficient immunoassay for the B cell help function of SARS-CoV-2-specific memory CD4+ T cells. *Cell Reports Methods* **2**, 100224 (2022).
20. Finney, J. & Kelsoe, G. Continuous Culture of Mouse Primary B Lymphocytes by Forced Expression of *Bach2*. *The Journal of Immunology* **207**, 1478–1492 (2021).
21. Nojima, T. *et al.* In-vitro derived germinal centre B cells differentially generate memory B or plasma cells in vivo. *Nat Commun* **2**, 465 (2011).
22. Ritchie, M. E. *et al.* limma powers differential expression analyses for RNA-sequencing and microarray studies. *Nucleic Acids Res* **43**, e47–e47 (2015).
23. Savarin, C. *et al.* Astrocyte response to IFN-γ limits IL-6-mediated microglia activation and progressive autoimmune encephalomyelitis. *J Neuroinflammation* **12**, 1–14 (2015).
24. Hu, C.-F. *et al.* Microglial Nox2 Plays a Key Role in the Pathogenesis of Experimental Autoimmune Encephalomyelitis. *Front Immunol* **12**, (2021).
25. Hol, E. M. & Pekny, M. Glial fibrillary acidic protein (GFAP) and the astrocyte intermediate filament system in diseases of the central nervous system. *Curr Opin Cell Biol* **32**, 121–130 (2015).
26. Fabis, M. J., Scott, G. S., Kean, R. B., Koprowski, H. & Hooper, D. C. Loss of blood–brain barrier integrity in the spinal cord is common to experimental allergic encephalomyelitis in knockout mouse models. *Proceedings of the National Academy of Sciences* **104**, 5656–5661 (2007).
27. Bennett, J. *et al.* Blood–brain barrier disruption and enhanced vascular permeability in the multiple sclerosis model EAE. *J Neuroimmunol* **229**, 180–191 (2010).
28. Nitsch, L. *et al.* Astrocyte-specific expression of interleukin 23 leads to an aggravated phenotype and enhanced inflammatory response with B cell accumulation in the EAE model. *J Neuroinflammation* **18**, (2021).
29. Barclay, W. E. *et al.* The AIM2 inflammasome is activated in astrocytes during the late phase of EAE. *JCI Insight* **7**, (2022).
30. Janzer, R. C. & Raff, M. C. Astrocytes induce blood-brain barrier properties in endothelial cells. *Nature* **325**, 253–257 (1987).
31. Heithoff, B. P. *et al.* Astrocytes are necessary for blood-brain barrier maintenance in the adult mouse brain. *Glia* **69**, 436 (2021).
32. Kantzer, C. G. *et al.* ACSA-2 and GLAST classify subpopulations of multipotent and glial-restricted cerebellar precursors. *J Neurosci Res* **99**, 2228–2249 (2021).
33. G. Kantzer, C. *et al.* Anti-ACSA-2 defines a novel monoclonal antibody for prospective isolation of living neonatal and adult astrocytes. *Glia* **65**, 990–1004 (2017).
34. Langer, H. F. *et al.* Platelets contribute to the pathogenesis of experimental autoimmune encephalomyelitis. *Circ Res* **110**, 1202–1210 (2012).
35. Li, W. *et al.* Astrocyte-Derived TNF-α-Activated Platelets Promote Cerebral Ischemia/Reperfusion Injury by Regulating the RIP1/RIP3/AKT Signaling Pathway. *Mol Neurobiol* **59**, 5734 (2022).
36. Zhu, Y., Yan, X., Zhai, C., Yang, L. & Li, M. Association between risk of asthma and gene polymorphisms in CHI3L1 and CHIA: a systematic meta-analysis. *BMC Pulm Med* **17**, (2017).
37. Zheng, Q. *et al.* Siglec1 suppresses antiviral innate immune response by inducing TBK1 degradation via the ubiquitin ligase TRIM27. *Cell Research 2015 25:10* **25**, 1121–1136 (2015).
38. Saitoh, O. *et al.* Alternative splicing of RGS8 gene determines inhibitory function of receptor type-specific Gq signaling. *Proc Natl Acad Sci U S A* **99**, 10138–10143 (2002).
39. Chen, W. *et al.* GRIN1 mutation associated with intellectual disability alters NMDA receptor trafficking and function. *Journal of Human Genetics 2017 62:6* **62**, 589–597 (2017).
40. Müller, I. I. *et al.* Gremlin-1 inhibits macrophage migration inhibitory factor-dependent monocyte function and survival. *Int J Cardiol* **176**, 923–929 (2014).
41. Bhat, S. A. *et al.* Enhanced Akt/GSK-3β/CREB signaling mediates the anti-inflammatory actions of mGluR5 positive allosteric modulators in microglia and following traumatic brain injury in male mice. *J Neurochem* **156**, 225–248 (2021).
42. Byrnes, K. R. *et al.* Metabotropic glutamate receptor 5 activation inhibits microglial associated inflammation and neurotoxicity. *Glia* **57**, 550–560 (2009).
43. Cho, S., Muthukumar, A. K., Stork, T., Coutinho-Budd, J. C. & Freeman, M. R. Focal adhesion molecules regulate astrocyte morphology and glutamate transporters to suppress seizure-like behavior. *Proc Natl Acad Sci U S A* **115**, 11316–11321 (2018).
44. Hlavac, N. & VandeVord, P. J. Astrocyte mechano-activation by high-rate overpressure involves alterations in structural and junctional proteins. *Front Neurol* **10**, 99 (2019).
45. Lee, C. G. *et al.* Role of Chitin and Chitinase/Chitinase-Like Proteins in Inflammation, Tissue Remodeling, and Injury. *Annu Rev Physiol* **73**, 479–501 (2011).

46. Gil-Perotin, S. *et al.* Combined Cerebrospinal Fluid Neurofilament Light Chain Protein and Chitinase-3 Like-1 Levels in Defining Disease Course and Prognosis in Multiple Sclerosis. *Front Neurol* **10**, (2019).
47. Kang, Q., Li, L., Pang, Y., Zhu, W. & Meng, L. An update on Ym1 and its immunoregulatory role in diseases. *Front Immunol* **13**, (2022).
48. Sitcheran, R., Gupta, P., Fisher, P. B. & Baldwin, A. S. Positive and negative regulation of EAAT2 by NF-kappaB: a role for N-myc in TNFalpha-controlled repression. *EMBO J* **24**, 510–520 (2005).
49. Valentin-Torres, A. *et al.* Sustained TNF production by central nervous system infiltrating macrophages promotes progressive autoimmune encephalomyelitis. *J Neuroinflammation* **13**, (2016).
50. Kemanetzoglou, E. & Andreadou, E. CNS Demyelination with TNF-α Blockers. *Current Neurology and Neuroscience Reports* vol. 17 Preprint at https://doi.org/10.1007/s11910-017-0742-1 (2017).
51. Stackhouse, T. L. & Mishra, A. Neurovascular Coupling in Development and Disease: Focus on Astrocytes. *Frontiers in Cell and Developmental Biology* vol. 9 Preprint at https://doi.org/10.3389/fcell.2021.702832 (2021).
52. Liu, L. R., Liu, J. C., Bao, J. S., Bai, Q. Q. & Wang, G. Q. Interaction of Microglia and Astrocytes in the Neurovascular Unit. *Frontiers in Immunology* vol. 11 Preprint at https://doi.org/10.3389/fimmu.2020.01024 (2020).
53. Berthiaume, A.-A. *et al.* Dynamic Remodeling of Pericytes In Vivo Maintains Capillary Coverage in the Adult Mouse Brain. *Cell Rep* **22**, 8–16 (2018).
54. Watkins, S. *et al.* Disruption of astrocyte–vascular coupling and the blood–brain barrier by invading glioma cells. *Nat Commun* **5**, 4196 (2014).
55. Niu, J. *et al.* Aberrant oligodendroglial–vascular interactions disrupt the blood–brain barrier, triggering CNS inflammation. *Nat Neurosci* **22**, 709–718 (2019).
56. Koehler, R. C., Gebremedhin, D. & Harder, D. R. Role of astrocytes in cerebrovascular regulation. *J Appl Physiol* **100**, 307–317 (2006).
57. MacVicar, B. A. & Newman, E. A. Astrocyte Regulation of Blood Flow in the Brain. *Cold Spring Harb Perspect Biol* **7**, a020388 (2015).
58. Girouard, H. *et al.* Astrocytic endfoot Ca^{2+} and BK channels determine both arteriolar dilation and constriction. *Proceedings of the National Academy of Sciences* **107**, 3811–3816 (2010).
59. Kaplan, L., Chow, B. W. & Gu, C. Neuronal regulation of the blood–brain barrier and neurovascular coupling. *Nat Rev Neurosci* **21**, 416 (2020).
60. Clifford, D. B. *et al.* Rituximab-associated progressive multifocal leukoencephalopathy in rheumatoid arthritis. *Arch Neurol* **68**, 1156–64 (2011).
61. von Büdingen, H.-C. *et al.* Onset of secondary progressive MS after long-term rituximab therapy - a case report. *Ann Clin Transl Neurol* **4**, 46–52 (2017).
62. Hawker, K. *et al.* Rituximab in patients with primary progressive multiple sclerosis: Results of a randomized double-blind placebo-controlled multicenter trial. *Ann Neurol* **66**, 460–471 (2009).
63. Yi, W., Schlüter, D. & Wang, X. Astrocytes in multiple sclerosis and experimental autoimmune encephalomyelitis: Star-shaped cells illuminating the darkness of CNS autoimmunity. *Brain, Behavior, and Immunity* vol. 80 10–24 Preprint at https://doi.org/10.1016/j.bbi.2019.05.029 (2019).
64. JL, W. *et al.* Astrocyte-T cell crosstalk regulates region-specific neuroinflammation. *Glia* **68**, 1361–1374 (2020).
65. Absinta, M. *et al.* A lymphocyte-microglia-astrocyte axis in chronic active multiple sclerosis. *Nature* **597**, 709–714 (2021).
66. Haider, L. *et al.* Multiple sclerosis deep grey matter: The relation between demyelination, neurodegeneration, inflammation and iron. *J Neurol Neurosurg Psychiatry* **85**, 1386–1395 (2014).
67. Mathiisen, T. M., Lehre, K. P., Danbolt, N. C. & Ottersen, O. P. The perivascular astroglial sheath provides a complete covering of the brain microvessels: An electron microscopic 3D reconstruction. *Glia* **58**, 1094–1103 (2010).
68. Cashion, J. M., Young, K. M. & Sutherland, B. A. How does neurovascular unit dysfunction contribute to multiple sclerosis? *Neurobiol Dis* 106028 (2023) doi:10.1016/J.NBD.2023.106028.
69. Vestergaard, M. B., Frederiksen, J. L., Larsson, H. B. W. & Cramer, S. P. Cerebrovascular Reactivity and Neurovascular Coupling in Multiple Sclerosis—A Systematic Review. *Front Neurol* **13**, 912828 (2022).
70. Aharoni, R., Eilam, R. & Arnon, R. Astrocytes in Multiple Sclerosis—Essential Constituents with Diverse Multifaceted Functions. *Int J Mol Sci* **22**, 5904 (2021).
71. Badimon, A. *et al.* Negative feedback control of neuronal activity by microglia. *Nature 2020 586:7829* **586**, 417–423 (2020).
72. Ponath, G. *et al.* Myelin phagocytosis by astrocytes after myelin damage promotes lesion pathology. *Brain* **140**, 399–413 (2017).
73. Chu, T. *et al.* Dynamic response of microglia/macrophage polarization following demyelination in mice. *J Neuroinflammation* **16**, 188 (2019).
74. Lisak, R. P. *et al.* B cells from patients with multiple sclerosis induce cell death via apoptosis in neurons in vitro. *J Neuroimmunol* **309**, 88–99 (2017).
75. Lisak, R. P. *et al.* Secretory products of multiple sclerosis B cells are cytotoxic to oligodendroglia in vitro. *J Neuroimmunol* **246**, 85–95 (2012).